Master Thesis
TVVR 26/5007
ISSN 1101-9824

Assessing Complex Water Quality Conditions Relevant to Ballast Water Operations in the Port of Hamburg

Environmental Context for Ballast Water Treatment Operations

Monireh Khazaei

Division of Water Resources Engineering
Department of Building and Environmental Technology
Lund University

Assessing Complex Water Quality Conditions Relevant to Ballast Water Operations in the Port of Hamburg

Environmental Context for Ballast Water Treatment Operations

By:
Monireh Khazaei

Master Thesis

Division of Water Resources Engineering
Department of Building & Environmental Technology
Lund University
Box 118
221 00 Lund, Sweden

Water Resources Engineering
TVVR 26/5007
ISSN 1101-9824

Lund 2026
www.tvrl.lth.se

Master Thesis
Division of Water Resources Engineering
Department of Building & Environmental Technology
Lund University

Swedish title:	Bedömning av komplexa vattenkvalitetsförhållanden med relevans för ballastvattenoperationer i Hamburgs hamn
English title:	Assessing Complex Water Quality Conditions Relevant to Ballast Water Operations in the Port of Hamburg
Author(s):	Monireh Khazaei
Supervisor:	Jing Li, Behshid Khodaei, Khanssa Lagdami, Camilla Hedberg, Jingjie Zhang
Examiner:	Magnus Larson
Language	English
Year:	2026
Keywords:	Ballast water management; challenging water quality; total suspended solids; turbidity; Sentinel-2; NDTI; Port of Hamburg; estuarine sediment dynamics

To the people of my country,

whose resilience and hope continue to inspire me.

Acknowledgements

I am very grateful to my main supervisor, Jing Li, for her guidance and feedback throughout this thesis. I would also like to thank Khanssa Lagdami and Jingjie Zhang for their support and helpful discussions during the thesis process.

I am especially thankful to Behshid Khodaei for her helpful guidance and discussions on the satellite-data analysis part of the thesis.

I am also grateful to Camilla Hedberg from Alfa Laval for her support, practical insights, and for arranging and participating in the field visit. The field visit provided valuable context for understanding ballast water treatment systems and their operational relevance.

I would also like to thank Alfa Laval for linking this thesis to practical questions in ballast water treatment. I acknowledge the organizations that provided the environmental and satellite data used in this study, including FGG Elbe, Hamburg Port Authority, GRDC, DWD, and the Copernicus/Sentinel-2 programme.

Finally, I would like to thank my family and friends for their patience, encouragement, and support throughout my master's studies.

Abstract

In estuarine ports, ballast water operations can be affected by short-term changes in water quality, especially when suspended sediment concentrations increase. This thesis assesses turbidity-related water-quality conditions relevant to ballast water operations in the Port of Hamburg, focusing on Seemannshöft during 2018–2024. Because direct total suspended solids (TSS) measurements were limited, a local turbidity–TSS relationship was developed and used to estimate daily TSS from the longer turbidity record.

The estimated TSS series was analysed for temporal and seasonal variability, high-TSS events, and relationships with environmental drivers, while Sentinel-2-derived Normalized Difference Turbidity Index (NDTI) was evaluated as complementary spatial information. Results showed generally moderate TSS-related conditions, interrupted by rare elevated events. Only 16 daily observations exceeded the 80 mg/L screening threshold, representing 0.71% of the record. Air temperature, wind speed, water level, upstream discharge, rainfall, and electrical conductivity explained only part of the variability. Supplementary prediction tests showed that short-term turbidity prediction improved mainly when recent turbidity observations were included, indicating strong temporal persistence in the Hamburg estuarine system.

Sentinel-2-derived NDTI provided useful complementary spatial information. A multi-year P95 hotspot-frequency analysis showed spatially heterogeneous elevated optical turbidity signals, although NDTI could not replace station-based TSS measurements. Overall, challenging suspended-sediment conditions mainly occurred as short events, supporting local measurements, event-based screening, and operational awareness rather than reliance on average seasonal conditions or environmental variables alone.

Sammanfattning

Ballastvatten används av fartyg för att hålla fartyget stabilt vid lastning, lossning och transport. I hamnar där vattenkvaliteten varierar snabbt kan behandling av ballastvatten bli svårare, särskilt när mängden suspenderat material i vattnet ökar. Den här studien undersöker turbiditetsrelaterade vattenkvalitetsförhållanden som kan vara relevanta för ballastvattenoperationer i Hamburgs hamn, med fokus på stationen Seemannshöft under perioden 2018–2024.

Studien använder data om turbiditet, totalt suspenderat material (TSS), miljövariabler och satellitbaserat NDTI från Sentinel-2. Eftersom direkta TSS-mätningar var begränsade användes ett lokalt samband mellan turbiditet och uppmätt TSS för att beräkna ungefärliga dagliga TSS-värden. Resultaten visar att TSS-relaterade förhållanden oftast var måttliga, men att korta perioder med högre värden förekom. Totalt låg 16 dagliga värden över screeninggränsen 80 mg/L, vilket motsvarar 0,71 % av alla dagliga värden.

Temperatur, vind, vattennivå, uppströms vattenföring och nederbörd förklarade bara en del av variationen. Kompletterande prediktionstester visade att korttidsprognoser för turbiditet främst förbättrades när tidigare turbiditetsvärden inkluderades, medan miljövariablerna gav ytterligare men begränsad prediktiv information. Elektrisk konduktivitet visade ett svagt till måttligt positivt samband och användes som en kompletterande indikator kopplad till salthalt.

Sentinel-2-baserat NDTI gav användbar rumslig information. En flerårig P95-hotspotfrekvensanalys visade att återkommande förhöjda optiska turbiditetssignaler var rumsligt varierande inom hamnområdet. NDTI kunde dock inte ersätta direkta TSS-mätningar. Studien visar att komplexa sedimentrelaterade vattenförhållanden främst uppträdde som kortvariga händelser, vilket stödjer lokal mätning, händelsebaserad screening och operativ medvetenhet snarare än bedömning utifrån genomsnittliga säsongsförhållanden eller enbart miljövariabler.

Table of contents

Background

Ships use ballast water to maintain stability during cargo operations and navigation. However, ballast water can also transport organisms from one aquatic environment to another. Organisms taken up in one port may survive the voyage and be discharged elsewhere, which has made ballast water an important pathway for biological invasions and a focus of international regulation (Casas-Monroy et al., 2022; David et al., 2026).

To reduce these risks, the International Maritime Organization introduced the Ballast Water Management Convention, which requires ships to manage ballast water and comply with discharge standards through ballast water management systems (IMO, 2018; Lloyd's Register, 2018).

The effectiveness of such systems, however, may be influenced by local water quality conditions. In particular, elevated turbidity and high concentrations of suspended particles can reduce the efficiency of treatment processes such as filtration and ultraviolet disinfection, making these conditions operationally challenging for ballast water treatment (Duan et al., 2023; Wang et al., 2025).

These problems are not only theoretical. The INTERTANKO database on ports with challenging water quality includes reports of reduced treatment rates, bypass events, operational limits, and system failures. Hamburg is listed in this database, which makes it a relevant case for examining suspended-sediment conditions in an operational port setting (INTERTANKO, 2026).

Estuarine ports are particularly complex because river flow, tides, sediment transport, and resuspension can change water quality over short time scales. As a result, turbidity and suspended matter may vary strongly within the same port area and over time (Wan & Wang, 2018; Zhu et al., 2021; North et al., 2004).

The Port of Hamburg was selected as a case study because it is a large estuarine port where ballast-water operations take place under dynamic water-quality conditions. It lies within the lower Elbe Estuary, where tidal dynamics, river inflow, sediment transport, dredging-related disturbance, and intensive navigation can all affect turbidity and suspended-sediment conditions. These characteristics make Hamburg a suitable setting for assessing particle-rich water-quality conditions relevant to ballast-water operational awareness (Hamburg Port Authority, n.d.; Dedeck, 2022).

Previous estuarine studies have shown that suspended-sediment variability is controlled by the interaction of river discharge, tidal forcing, mixing, sediment availability, and local resuspension processes. In estuaries, these processes can produce strong temporal and spatial variability in turbidity and suspended matter, especially in areas affected by tidal propagation and morphological change. This context is relevant for the Port of Hamburg because it is located within a dynamic estuarine system where local water-quality conditions may change over short timescales (Dyer, 1997; Winterwerp & van Kesteren, 2004; Grabemann & Krause, 2001; Dedeck, 2022).

Previous studies have addressed ballast water treatment technologies, compliance challenges, and estuarine turbidity dynamics. However, less attention has been given to how local turbidity and suspended-sediment conditions in an operational port may affect the practical context of ballast water operations (Outinen et al., 2024; Casas-Monroy et al., 2022; Wang et al., 2025).

This thesis therefore uses available in-situ, environmental, and satellite-derived data to assess turbidity-related water quality conditions in the Port of Hamburg. The main focus is on TSS variability, elevated events, and the usefulness of Sentinel-2 derived NDTI as supporting spatial information (Gorelick et al., 2017; Lee et al., 2021; Chowdhury et al., 2023). The availability of long-term monitoring data at Seemannshöft also made it possible to examine temporal variability and elevated TSS events over several years.

The aim is not to directly evaluate ballast water treatment system performance, but to provide an environmental assessment that is relevant to ballast water operations in a dynamic estuarine setting. Instead, the analysis provides screening-level information on when and where particle-rich water-quality conditions may occur, which can support operational awareness for ballast-water uptake, treatment planning, and monitoring needs.

Although the wider project relates to monitoring and modelling of suspended-sediment hotspots, this thesis focuses on the observational part. It uses available measurement and satellite datasets to identify when and where suspended-sediment conditions may become relevant for ballast water operations.

The thesis followed a stepwise observational approach. First, station-based turbidity and measured TSS observations were matched to develop a local turbidity–TSS relationship. This relationship was then used to estimate daily TSS from the longer turbidity record. The estimated TSS series was analysed to identify temporal patterns, seasonal variation, and high-TSS events.

Environmental variables and upstream discharge were then used to examine possible drivers, while Sentinel-2-derived NDTI was used as complementary spatial information. This approach was designed to assess challenging water-quality conditions from available monitoring and satellite data, rather than to develop a full process-based or operational prediction model.

In this context, turbidity and TSS were used as screening indicators rather than direct measures of BWMS performance. Particle-rich water may increase filtration load, maintenance needs, and operational complexity, while UV transmittance can also be affected by dissolved materials. The aim was therefore to identify when and where such challenging water-quality conditions may be relevant for operational awareness.

Literature Review

2.1 Ballast Water and the Spread of Aquatic Organisms

Ballast water is a well-known pathway for moving aquatic organisms between marine and estuarine environments. During normal ship operations, water taken up in one port may carry bacteria, phytoplankton, zooplankton, or small invertebrates to another region (IMO, 2018; David et al., 2026).

Some of these organisms may survive the voyage and establish in new environments after discharge, where they can alter local ecosystems and create ecological as well as economic impacts. Reported consequences include changes in biodiversity, disturbance of ecosystem functioning, and damage to fisheries and coastal infrastructure (David et al., 2026).

Ballast water management is therefore both an operational requirement for shipping and an environmental protection measure. The main concern is not only the amount of water moved, but the possibility that viable organisms are transported across natural biogeographical barriers.

2.2 International Regulations and the Ballast Water Management Convention

The risks linked to ballast water discharge led to the adoption of the International Convention for the Control and Management of Ships' Ballast Water and Sediments, usually referred to as the Ballast Water Management Convention (IMO, 2018).

Since its entry into force, the Ballast Water Management Convention has required internationally operating ships to manage ballast water either by exchange procedures or by using approved treatment systems, depending on the applicable compliance requirements (IMO, 2018; Lloyd's Register, 2018).

Within this framework, the D-1 standard historically referred to ballast water exchange, where coastal ballast water was replaced with open-ocean water during voyages. However, from 8 September 2024, D-1 is no longer available as the main compliance option for most ships, and ships are required to meet the D-2 discharge performance standard. The D-2 standard sets limits for viable organisms and indicator microbes in treated ballast water. In practice, this means that onboard ballast water management systems are now central for regulatory compliance under operating conditions (IMO, 2024).

To support implementation of the Convention, IMO has also issued interim guidance for ships operating in challenging water-quality conditions, including resolution MEPC.387(81). This is relevant to the present thesis because variable turbidity and suspended-sediment conditions may indicate particle-rich water, which can create operational challenges for ballast water management systems. Therefore, several studies have highlighted that achieving consistent compliance under real operating conditions may remain challenging, especially when treatment systems are exposed to variable environmental conditions (Outinen et al., 2024; Wang et al., 2025).

For this reason, the regulatory context is directly relevant to studies of challenging water quality, as local environmental conditions may affect how ballast water treatment systems perform in practice.

Industry guidance also shows that operational decisions matter under challenging water quality conditions. The INTERTANKO CWQ database reports cases where ships experienced reduced treatment rates, bypass events, operational limits, or system failures in specific ports (INTERTANKO, 2026).

2.3 Ballast Water Treatment Technologies

Compliance with the D-2 standard is commonly achieved using onboard treatment systems that combine physical removal and organism inactivation processes, such as filtration, UV irradiation, or electrochemical treatment (Duan et al., 2023; Dong et al., 2023).

Many ballast water management systems use filtration as an initial treatment step before the main disinfection stage. This can include systems based on UV treatment, electrochlorination, chemical injection, or other disinfection processes. In particle-rich water, filtration may become operationally more demanding because more suspended material has to be removed or managed by the system. This can increase the need for cleaning, backwashing, or maintenance, depending on the system design and operating conditions (Dong et al., 2023; Outinen et al., 2024).

In addition to bulk TSS concentration, particle characteristics such as particle size and particle load may also influence filtration performance and the operational challenge posed by particle-rich water.

Shipboard studies also show that treatment performance in practice may differ from performance under controlled test conditions. In ports, particle concentrations, salinity, and other environmental conditions can change quickly. For this reason, local water quality needs to be considered when interpreting how ballast water treatment systems may perform in dynamic port environments (Dong et al., 2023; Outinen et al., 2024).

2.4 Environmental Factors Affecting Ballast Water Treatment

In estuarine ports, suspended sediment and turbidity conditions can vary strongly over time and space because river discharge, tidal forcing, sediment transport, and resuspension interact with local morphology (North et al., 2004; Wan & Wang, 2018; Zhu et al., 2021).

Such variability is directly relevant to ballast water treatment. High concentrations of suspended particles may reduce the effectiveness of filtration and limit ultraviolet light penetration, thereby decreasing treatment efficiency and potentially affecting compliance under operational conditions.

Industry reports confirm that challenging water quality can create practical problems for ships using BWMS. The INTERTANKO CWQ database includes reports of reduced treatment rates, bypass situations, operational limits, and system failures (INTERTANKO, 2026).

TSS is therefore a useful indicator in this study because it represents particle-rich conditions that may interfere with filtration and UV treatment. Other factors, such as salinity and temperature, may also influence ballast water treatment performance, particularly in electrochlorination-based systems (Duan et al., 2023; Wang et al., 2025). However, suspended particles were the main focus of this thesis because turbidity and TSS were used as indicators of particle-rich water conditions.

TSS should therefore be treated as an important indicator of particle-rich water, but not as a complete description of suspended matter. Particle size, composition, concentration, and exposure duration can also influence the effect of suspended solids (Bilotta & Brazier, 2008).

This is especially important in large estuarine ports, where high turbidity may occur only during short events rather than as a constant background condition. For this reason, identifying the timing of elevated TSS events, and improving the ability to anticipate such events, may be more relevant for ballast-water operational awareness than considering average concentrations alone (North et al., 2004; Wang et al., 2021; Outinen et al., 2024).

Satellite observations can help monitor turbidity patterns in estuarine waters, especially where field-based measurements are sparse. In this thesis, satellite data are used only as supporting spatial information, not as a replacement for field measurements (Lee et al., 2021; Chowdhury et al., 2023; Nangir et al., 2025).

2.5 Hydrodynamic and Sediment Processes in Estuarine Systems

Hydrodynamic conditions control how water and sediment move through an estuary. River discharge, tides, estuarine shape, and local resuspension can all change the amount of suspended material in the water column (Chen et al., 2015; Torres-Bejarano et al., 2025).

These processes are important for this thesis because elevated TSS at Seemannshöft may not come from one source only. Suspended matter can arrive from upstream, but it can also be redistributed by tides, local resuspension, and sediment trapping within the estuary (Hesse et al., 2019; Zhu et al., 2021).

The Port of Hamburg is located within this dynamic part of the Elbe Estuary. Its water quality is affected by upstream discharge, tides, sediment transport, dredging, and navigation-related disturbance (Ohle et al., 2023; Dedeck, 2022).

These processes help explain why turbidity and TSS may change quickly at the study site, even though this thesis does not include hydrodynamic modelling. Although numerical models are often used to study estuarine sediment dynamics, this thesis focuses on observations and data analysis.

Overall, previous studies show that ballast water treatment can be affected by particle-rich water and that estuarine suspended sediment dynamics are highly variable. However, fewer studies connect local port-scale suspended-sediment variability, satellite-derived turbidity indicators, and practical screening needs for ballast water operations. This thesis addresses that gap using available monitoring and satellite data from the Port of Hamburg.

Materials and Methods

3.1 Study Area

The study area is located along the lower Elbe River in northern Germany. It includes the Port of Hamburg and the upstream reach towards Neu Darchau. This area is part of a tidal estuarine transition zone, where river discharge, tides, sediment transport, and port-related processes interact. Figure 3.1a shows the regional study area along the Elbe River, including the Port of Hamburg, Seemannshöft, Geesthacht, and Neu Darchau. Figure 3.1b provides a zoom-in view of the Port of Hamburg and the Seemannshöft monitoring station used in this thesis (Hamburg Port Authority, n.d.; Ohle et al., 2023).

Seemannshöft is located within the Port of Hamburg area along the tidal Elbe waterway. This location makes it suitable as the primary station for assessing local turbidity- and TSS-related conditions within the main port environment.

Figure 3.1a. *Regional study area along the lower Elbe River in northern Germany, including the Port of Hamburg, the Seemannshöft monitoring station, the upstream discharge reference station at Neu Darchau, and Geesthacht as an additional contextual Elbe monitoring location. Background map: OpenStreetMap.*

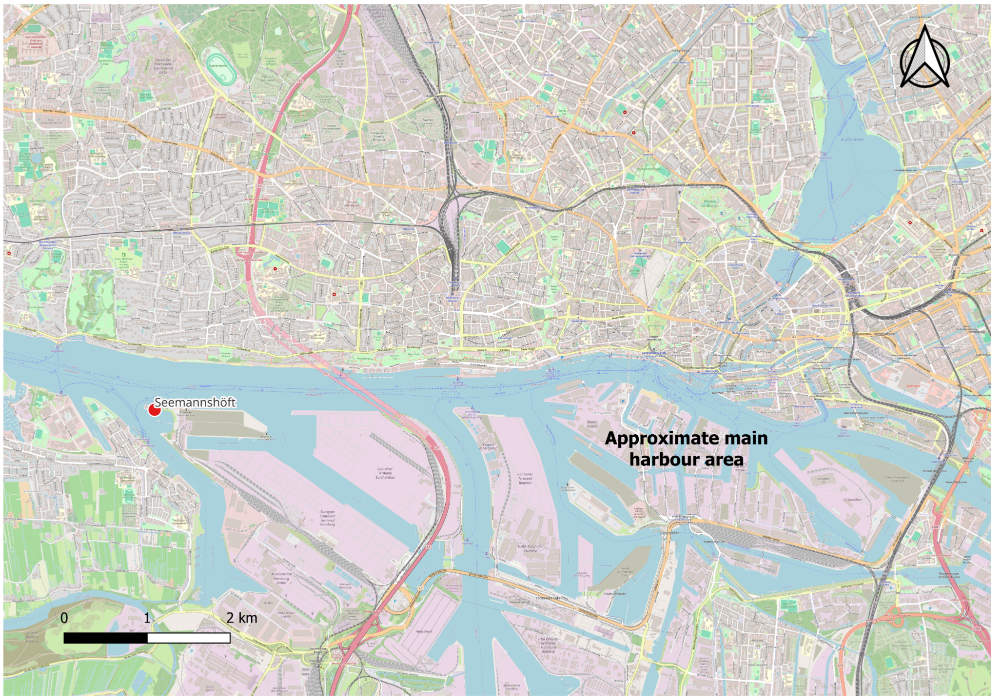

Figure 3.1b. *Local map of the Port of Hamburg showing the Seemannshöft monitoring station and the approximate main harbour area used for contextual interpretation. The map provides local harbour context and does not indicate observed ballast-water operation locations.*

The Port of Hamburg is the main focus of this study because it is important for navigation and ballast water operations. It also has variable water-quality conditions. The port lies within the Elbe Estuary and is affected by tides, upstream river discharge, sediment transport, navigation, and dredging-related resuspension. These processes can cause turbidity and suspended sediment to vary over time and space (Hamburg Port Authority, n.d.; Ohle et al., 2023; Dedeck, 2022).

The lower Elbe Estuary is strongly influenced by both river discharge and tidal forcing. The average tidal range in the Port of Hamburg is approximately 3.7 m, which produces regular changes in water level and tidal currents (Port of Hamburg, n.d.; Tideelbe, n.d.). The multi-year average runoff of the Elbe near the mouth is about 861 m^3/s, while discharge conditions vary seasonally and during high-flow events (IKSE, n.d.). These hydraulic conditions influence mixing, sediment transport, and the resuspension of fine material, and therefore provide important context for interpreting turbidity and suspended-sediment variability.

The operational complexity of the port is also reflected in the way hydrographic data are managed. The Hamburg Port Authority has its own hydrographic survey department, and hydrographic information is used to support harbour management and navigation-related planning (Köster, 2017).

Three monitoring stations were considered in the present study. Seemannshöft, located within the Hamburg port area, was used as the primary station for the main analysis of turbidity- and TSS-related variability. Neu Darchau was included as an upstream reference station for river discharge, providing supporting information on fluvial forcing within the broader Elbe system. Geesthacht was considered as an additional Elbe monitoring location in the study-area context, but it was not used as a core station in the main quantitative analysis. Together, these stations were used to describe local port conditions and the upstream hydrological context.

3.2 Materials and Methods

Because of data availability and the scope of a master thesis, no hydrodynamic or water-quality model was developed. Instead, the study uses observational data to assess turbidity-related water-quality conditions and to identify temporal and spatial hotspot indicators relevant to ballast water operations.

Table 3.1 summarizes the main monitoring stations and data sources used in the study, together with additional stations that were checked as possible backup sources for the turbidity–TSS relationship.

Table 3.1. *Monitoring stations and data sources used or checked in this study.*

Station / data source	Location / role	Variables	Use in thesis
Seemannshöft	Main monitoring station in the Port of Hamburg	Turbidity, TSS/filter residue, conductivity	Main water-quality analysis and turbidity–TSS relationship
Neu Darchau	Upstream Elbe hydrological station	River discharge	Upstream hydrological reference
Hamburg Port Authority / local port data	Port of Hamburg	Water level	Local hydrological driver
DWD / meteorological data	Hamburg area	Air temperature, wind speed	Environmental-driver analysis
Sentinel-2	Satellite imagery	NDTI / optical turbidity pattern	Spatial hotspot screening
Open-Meteo	Study-location weather data	Daily rainfall	Supplementary rainfall check
Hamburg WGMN stations, e.g. Blankenese and Bunthaus	Additional Hamburg monitoring stations	Recent turbidity values	Checked as possible backup, but not matched with TSS
FGG Elbe additional stations, e.g. Geesthacht, Teufelsbrück	Additional Elbe stations	Filter residue / TSS-type data	Checked as possible backup, but suitable matched turbidity–TSS pairs were not available

3.2.1 Data sources

This study used several environmental datasets for the lower Elbe River and the Port of Hamburg. The datasets included water quality, hydrometeorological data, and satellite-derived optical information. The main temporal analysis covered 2018–2024. Satellite-based spatial analysis was used to add information on the distribution of turbidity-related conditions. These data were used to assess suspended sediment variability and water-quality conditions relevant to ballast water operations.

The selected environmental variables were included to represent key physical and hydrological processes that may influence turbidity and suspended-sediment conditions in an estuarine port. Water level was used as an indicator of tidal and hydrodynamic forcing, river discharge as a proxy for freshwater inflow and sediment supply, wind speed as an indicator of wind-driven mixing and possible resuspension, and rainfall as a proxy for runoff-related inputs. Air temperature was included as a seasonal environmental indicator, while conductivity was used as a salinity-related proxy that may reflect estuarine mixing and particle behaviour (Dyer, 1997; Winterwerp & van Kesteren, 2004; Grabemann & Krause, 2001).

Monitoring-station water quality data, including turbidity and total suspended solids (TSS), were obtained from the FGG Elbe data portal for the Seemannshöft monitoring station and related Elbe stations (FGG Elbe, n.d.). Daily turbidity observations were used as the basis for estimating TSS through a site-specific empirical relationship between measured turbidity and TSS. Electrical conductivity at 25°C was also obtained from the FGG Elbe data portal and was used as a supplementary salinity-related proxy, because consistent direct salinity measurements were not available for the full study period.

River discharge data were collected for the Neu Darchau station from the Global Runoff Data Centre (GRDC, n.d.) and were used to represent upstream fluvial forcing within the broader Elbe system.

Meteorological data, including wind speed and air temperature, were obtained from the German Weather Service (DWD) for the Hamburg-Fuhlsbüttel station. These data were aggregated to daily values and used to examine whether atmospheric conditions were associated with estimated TSS variability. Water level data for Seemannshöft were obtained from the Hamburg Port Authority HydroOnline tide gauge service and were aggregated to daily mean values for comparison with estimated TSS.

Daily rainfall data were obtained from the Open-Meteo historical weather API for the Seemannshöft study location for 2018–2024. Rainfall was used as a supplementary predictor in the rainfall and forecast-window sensitivity checks.

Satellite data were accessed and processed in Google Earth Engine (GEE), using Sentinel-2 observations for the study area (Gorelick et al., 2017). The data were used to calculate the Normalized Difference Turbidity Index (NDTI). NDTI was then compared with available in-situ observations. In this study, NDTI was treated as a relative optical indicator of surface turbidity, not as a direct measurement of TSS.

Gridded salinity data from the Copernicus Marine Environment Monitoring Service were also reviewed. However, the selected product did not provide valid surface salinity values for the inner Hamburg Port and Seemannshöft grid cells. This was most likely due to land masking and model-resolution limitations. Therefore, salinity was not used as a main quantitative driver. Electrical conductivity was used instead as a station-based salinity-related proxy.

Geographic data processing, visualization, and map production were carried out in QGIS. Background spatial datasets, including basemaps and bathymetric information from EMODnet and national providers, were reviewed to describe the physical setting of the study area. These datasets were not used as core quantitative variables in the statistical analysis.

3.2.2 Station selection and analytical roles

Three monitoring stations were considered: Seemannshöft, Geesthacht, and Neu Darchau. They were used to represent local port conditions, upstream hydrological conditions, and supporting observations within the lower Elbe system.

Seemannshöft was the primary station in this study. It is located within the Port of Hamburg, which is the main area of interest for ballast water operations. The station provided the main in-situ data for analysing turbidity and TSS-related variability. It was used to examine temporal variation, monthly and seasonal patterns, distribution, hotspot occurrence, and relationships with environmental drivers. Geesthacht was kept as a supporting reference location in the study-area description. It was not used as a core station in the main quantitative analysis.

Neu Darchau was used as the upstream reference station for river discharge. Its discharge data provided information on fluvial forcing in the broader Elbe system. The data were used to support the interpretation of temporal TSS variability. However, discharge was not treated as the main explanatory variable in the core analysis.

Local port-related processes, including navigation, dredging, and potential ship-induced sediment resuspension, were considered as possible contributors to turbidity variability. However, these processes were not analysed quantitatively because suitable high-resolution operational datasets, such as vessel traffic or AIS data, propeller characteristics, berth-level operation records, dredging activity logs, and harbour-basin-scale hydrodynamic data, were not available within the scope of this thesis.

Therefore, ship-induced resuspension was treated as a qualitative contextual factor in the interpretation of the results rather than as a modelled or statistically tested driver.

3.2.3 Data preprocessing

Before the analysis, all datasets were pre-processed in Python. Dates and times from the different sources were converted to a standard datetime format using pandas. A common date-only variable was then created. This made it possible to compare datasets with different temporal resolutions, including field observations, satellite data, and environmental variables.

The in-situ water-quality datasets were checked for missing values, duplicate records, inconsistent formatting, and non-numeric values. Turbidity, TSS, electrical conductivity, water level, wind speed, and temperature were converted to numeric format when needed. Invalid or missing records were removed from the analytical datasets. Environmental variables with higher temporal resolution were aggregated to daily values before comparison with estimated TSS.

Satellite-derived data were processed separately. Cloud contamination, water masking, and valid Sentinel-2 coverage were checked before the NDTI analysis. Only valid water pixels and cloud-filtered observations were kept. Negative NDTI values were not removed automatically, because NDTI is a relative optical index and can include both positive and negative values. Observations were excluded only when they were affected by masking, missing data, or non-water conditions.

After cleaning, the datasets were merged using the common date variable. Exact-date matching was used for in-situ and environmental comparisons. Station-based and satellite-derived data comparisons followed the matching approach described in the next sections. These steps made the datasets consistent enough for the statistical, temporal, seasonal, hotspot, and satellite-based analyses.

Basic data inspection was carried out before analysis, including checks of missing values, duplicate records, data types, date consistency, and summary statistics.

3.2.4 TSS estimation and statistical analyses

The relationship between local monitoring turbidity and measured TSS at Seemannshöft was examined using simple linear regression. Only observations from matching measurement dates were used. The resulting station-specific regression was applied to the longer daily turbidity record. This allowed TSS to be estimated for days with available turbidity observations. The estimated series extended the temporal analysis while keeping a link to measured station-based TSS data.

The estimated TSS values were used in the temporal, seasonal, distribution, hotspot, and environmental-driver analyses. The turbidity–TSS regression had only moderate explanatory power. Therefore, the estimated TSS values were treated as indicative TSS-related values, not as exact replacements for direct TSS measurements.

To further assess the robustness of the turbidity–TSS relationship, three supplementary checks were carried out using the matched measured turbidity and measured TSS observations. First, the matched turbidity and TSS observations were plotted as time series to examine whether both variables showed similar temporal behaviour and whether seasonal or event-related patterns were visible. Second, a log-transformed regression was tested using log-transformed turbidity and log-transformed TSS.

This was done because the original scatter plot showed considerable spread at higher values, and log transformation can reduce the influence of high-value observations and heteroscedasticity. Third, the matched dataset was divided into winter and summer groups to examine whether the turbidity–TSS relationship differed between seasons. These supplementary analyses were used to interpret the uncertainty of the TSS estimation and to assess whether a single annual regression was sufficient.

Exploratory statistical analyses were used to examine associations between estimated TSS and selected environmental variables. The variables were daily mean air temperature, daily mean wind speed, daily mean water level, electrical conductivity at 25°C, and river discharge at Neu Darchau. Air temperature, wind speed, and water level were compared directly with estimated TSS at Seemannshöft using exact-date matching.

Electrical conductivity was used as a supplementary salinity-related proxy. River discharge at Neu Darchau was used as an upstream hydrological reference, not as a direct local predictor of TSS at Seemannshöft.

Correlation analysis and simple linear regression were used to describe the direction and strength of the relationships. Pearson's r was used for linear relationships. Spearman's ρ was used for monotonic relationships based on ranked values. Both coefficients range from −1 to +1. Values close to zero indicate weak or no association. The results were interpreted as associations, not causal relationships.

As an additional sensitivity check, measured turbidity was log-transformed and analysed using multiple linear regression with the available environmental variables as predictors. The model included daily mean air temperature, daily mean wind speed, daily mean water level, and river discharge at Neu Darchau.

This analysis was used to test whether the combined environmental parameters explained turbidity variability better than the individual pairwise relationships. Electrical conductivity was not included in this multivariable model because substantially fewer matched observations were available. The final matched dataset used for this analysis is summarized in Table B1 in Appendix B, and the observed-versus-predicted diagnostic plot is shown in Figure B1.

To provide an initial overview of temporal variability and possible event-based behaviour, the main variables used in the exploratory environmental analysis were also visualized as time series.

In addition, an exploratory Random Forest regression was tested to assess the relative importance of the environmental variables under a non-linear modelling approach. The Random Forest model used log-transformed turbidity as the response variable and daily mean air temperature, daily mean wind speed, daily mean water level, and Neu Darchau discharge as predictors.

The dataset was split into 75% training data and 25% test data, and model performance was also evaluated using five-fold cross-validation. The model was fitted with 500 trees, and feature importance was used to assess the relative contribution of each predictor. The Random Forest result was interpreted as an exploratory sensitivity check and was not used as an operational prediction model.

A time-ordered prediction test was also carried out to evaluate short-term predictability. The models were trained on data from 2018–2022 and tested on 2023. Lagged turbidity and lagged environmental variables were included to examine whether previous conditions improved prediction compared with same-day environmental variables alone. This analysis was used to distinguish between predictability based on environmental drivers and predictability based on temporal persistence in turbidity.

The modelling workflow included time-series visualization of the main variables, correlation analysis, lag-feature testing, a time-ordered train-test split, and comparison of Linear Regression, Random Forest, XGBoost, and a simple ARIMA(1,0,0) baseline.

Linear Regression, Random Forest, XGBoost, and a simple ARIMA(1,0,0) baseline were compared using the same 2023 test period. The ARIMA model was included only as a simple autoregressive baseline and was not optimized further.

A log-transformed regression was also tested as a diagnostic check because turbidity and TSS data are commonly right-skewed and may include a small number of high-value observations. Log transformation can reduce the influence of extreme values and help assess whether the relationship becomes more linear on a transformed scale. In this study, the log-transformed model did not improve the explanatory power compared with the simple linear model, so the linear regression was retained for the main TSS estimation.

Satellite-derived NDTI was analysed separately as a relative optical indicator of surface turbidity. NDTI was compared with station-based observations using matched dates where available. These comparisons were treated as consistency checks, not as full validation of satellite-derived TSS estimates.

Principal Component Analysis (PCA) was also applied to the standardized environmental variables to explore whether common patterns among discharge, water level, wind speed, and air temperature could summarize the environmental variability and provide additional context for turbidity variability.

To further clarify the short-term forecasting setup, a supplementary Random Forest forecast-window check was performed. The target variable was log-transformed turbidity. The input variables were lagged log-transformed turbidity, air temperature, wind speed, water level, discharge, and rainfall.

These inputs were selected to test whether turbidity prediction was mainly driven by recent turbidity persistence or by previous environmental conditions. Input windows of 7, 14, and 21 previous days were tested for predicting log-transformed turbidity 1, 2, and 3 days ahead. The data were split chronologically into training data from 2018–2021, validation data from 2022, and an independent test period in 2023. The validation period was used to compare model setups, while the 2023 test period was used for final evaluation.

3.2.5 Satellite–in-situ comparison

Satellite-derived observations were compared with available in-situ measurements at Seemannshöft. The aim was to check whether remotely sensed optical information could support the analysis of turbidity-related conditions. The satellite analysis used Sentinel-2-derived NDTI. NDTI was treated as a relative indicator of surface turbidity, not as a direct estimate of TSS.

NDTI was calculated as (Red − Green) / (Red + Green), using Sentinel-2 Band 4 (red) and Band 3 (green). In band notation, this corresponds to (B4 − B3) / (B4 + B3). The index was used only as a relative optical indicator of surface turbidity and was not converted directly to TSS concentration. A direct satellite-based TSS retrieval would require local calibration and validation using spatially and temporally matched in-situ TSS measurements, which were not available across the port area in this study.

Sentinel-2 observations for 2018–2024 were accessed and processed in Google Earth Engine (GEE) (Gorelick et al., 2017). NDTI values were extracted for the Seemannshöft water-only polygon after cloud filtering and water masking. The extracted NDTI values were then compared with available measured turbidity and TSS/filter residue measurements from the FGG Elbe data portal.

Exact-date matching was used to compare NDTI with in-situ observations. The NDTI–turbidity comparison had more matched observations because turbidity was measured more frequently. The NDTI–TSS/filter residue comparison was more limited because TSS/filter residue measurements were less frequent.

The relationships between NDTI and station-based observations were evaluated using correlation analysis and simple linear regression. Pearson correlation was used for linear association. Spearman rank correlation was used for monotonic association. The aim was not to develop a universal satellite-based TSS model. Instead, the aim was to evaluate whether NDTI captured relative variability in surface turbidity conditions at Seemannshöft.

In addition to the station-based satellite–in-situ comparison, a spatial NDTI screening analysis was carried out across the Port of Hamburg. Sentinel-2 observations from 2018–2024 were cloud-filtered and masked to retain water pixels only. After preprocessing, 273 valid Sentinel-2 observations were retained. Mean and percentile-based spatial NDTI products were generated, including mean NDTI and P90 NDTI maps.

A hotspot-frequency analysis was then performed using a stricter P95 NDTI threshold. The port-scale P90 and P95 NDTI thresholds were 0.00455 and 0.01636, respectively, derived from the spatial mean of the pixel-wise percentile images. For the hotspot-frequency analysis, each valid Sentinel-2 observation was classified pixel by pixel. Pixels with NDTI values above the port-scale P95 threshold were classified as high-NDTI observations.

Hotspot frequency was then calculated as the percentage of valid observations exceeding this threshold. Pixels with fewer than 20 valid observations during the study period were excluded to reduce uncertainty caused by sparse satellite coverage. A 150 m focal mean was applied to the hotspot-frequency raster to reduce pixel-level speckle and improve spatial interpretability. The resulting map was interpreted as a relative optical turbidity hotspot-frequency product, not as a direct TSS exceedance map or a direct measurement of ballast-water treatment risk.

3.2.6 Identification of elevated estimated TSS events

The daily estimated TSS time series at Seemannshöft for 2018–2024 was examined to identify periods with clearly elevated suspended-sediment conditions. In this study, elevated estimated TSS event days were defined as days when estimated TSS exceeded 80 mg/L.

The 80 mg/L value was used as a practical screening threshold to identify the upper range of estimated TSS conditions in the available daily record. It was not intended to represent a regulatory limit, a BWMS treatment limit, or a universal operational threshold. Instead, it was used to separate clearly elevated estimated TSS conditions from more common background variability and to support event-based screening.

The threshold was also supported by suspended-sediment impact literature. Griffiths and Walton (1978), as summarized in the U.S. EPA report on suspended and bedded sediment criteria, reported an upper tolerance range of about 80–100 mg/L for fish (U.S. EPA, 2006). In this thesis, the 80 mg/L value was therefore used only as a conservative supporting reference for screening episodic high-TSS conditions, not as a biological or ballast-water treatment limit.

Because no system-specific operational TSS threshold was available, the 80 mg/L threshold was interpreted only as a screening criterion for potentially challenging particle-rich water conditions. To evaluate the sensitivity of the results to this threshold choice, additional thresholds of 70 mg/L and 90 mg/L were also tested.

The analysis was applied to the daily estimated TSS record to identify the timing, frequency, and grouping of elevated events. This helped indicate whether elevated estimated TSS values occurred as isolated single-day events or as short grouped events, which may be relevant for ballast-water operational awareness.

This station-based temporal exceedance analysis is separate from the satellite-based spatial NDTI hotspot-frequency analysis, which was based on relative optical NDTI thresholds rather than estimated TSS concentrations.

3.2.7 Software and visualization

Data processing, statistical analysis, and visualization were mainly carried out in Python. The workflow included data cleaning, temporal matching, daily aggregation, regression analysis, correlation analysis, elevated-event identification and spatial hotspot-frequency mapping. Figures included time series plots, scatter plots, histograms, bar charts, and seasonal boxplots. Python helped keep the workflow consistent and reproducible across the different datasets.

Google Earth Engine was used for accessing, filtering, and processing Sentinel-2 imagery and for deriving satellite-based NDTI values. QGIS was used for spatial visualization, map production, and final layout preparation of spatial outputs, including the study area map and the satellite-derived NDTI hotspot-frequency map. This included basemap overlay, legend preparation, scale bar and north arrow placement, and export of thesis figures. Together, Python, Google Earth Engine, and QGIS were used to combine in-situ observations, environmental data, and satellite-derived information.

3.2.8 Field visit and practical system context

In addition to the quantitative datasets analysed in this study, a field visit to an onboard UV-based ballast water treatment system was conducted to provide qualitative operational context. The visit was used to improve understanding of the treatment train and to support the practical interpretation of treatment-related challenges under particle-rich water conditions. Observations from the visit were not treated as a formal dataset and were not included in the quantitative statistical analysis.

The observed system was a UV-based ballast water treatment system with a treatment capacity of 500 m^3/h. It was located in the engine room and included an automatic filter, a UV unit, pumps, and a digital control interface. Operation could be monitored and controlled locally through the human–machine interface in the engine room or remotely from the control room.

Figure 3.2. Overview screen of the onboard UV-based ballast water treatment system observed during the field visit, showing the main treatment components, including the filter, UV reactor, and cleaning/CIP loop.

The treatment train consisted of filtration followed by UV treatment. In addition, the UV unit included a separate cleaning-in-place (CIP) system for the quartz sleeves, which may become fouled during ballast water treatment.

The filtration system used an automatic filter with a mesh size of approximately 20 µm, and backwashing was activated when the differential pressure reach 0.3 bar. Under particle-rich conditions, increased filter loading may therefore require more frequent or extended backwash cycles.

The field discussion indicated that high turbidity alone was not necessarily the main operational concern. Instead, high TSS conditions and particle characteristics, including particle size and particle load, were considered more relevant for potential treatment challenges. The observed vessel had not experienced challenging water quality during operation, but similar challenges had been reported for other vessels. Therefore, the field visit was interpreted as practical context rather than direct evidence of BWMS performance under challenging water-quality conditions.

For UV-based treatment, the discussion highlighted the importance of maintaining sufficient UV intensity and keeping the quartz sleeves clean. The field visit helped connect the quantitative results to practical ballast-water treatment conditions.

The observations were qualitative and vessel-specific, and they should not be interpreted as a formal performance assessment. However, they helped clarify why short periods of particle-rich water may be operationally relevant for filtration and UV-based treatment stages.

Results

4.1 Relationship between turbidity and TSS

Measured turbidity values were compared with measured total suspended solids (TSS) at Seemannshöft. This was done to develop a local basis for estimating TSS. Only observations with matching measurement dates were used. The relationship is shown in Figure 4.1.

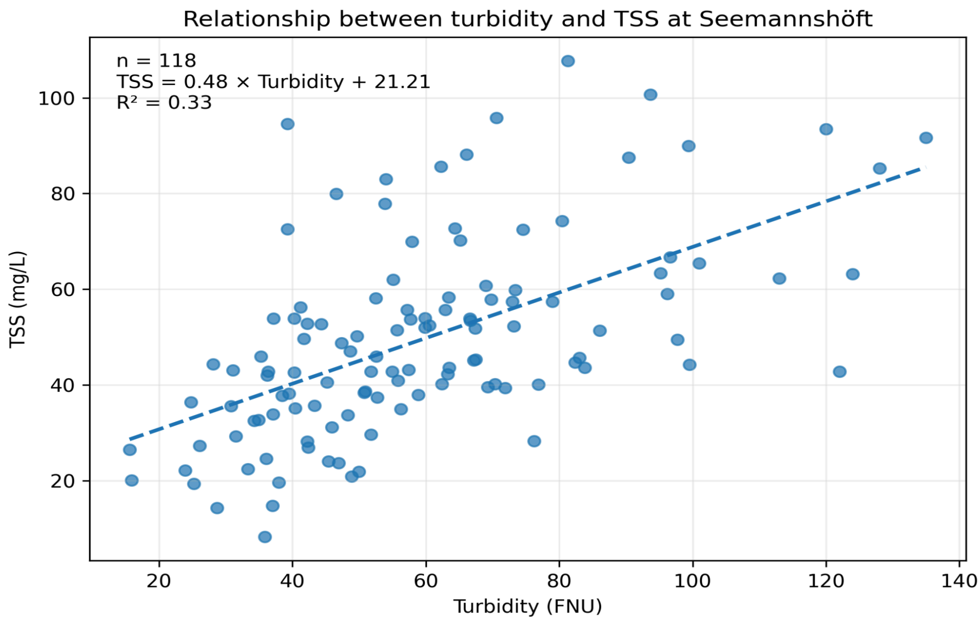

Figure 4.1. *Relationship between turbidity (FNU) and total suspended solids (TSS, mg/L) at the Seemannshöft station. The dashed line represents the linear regression model (TSS = 0.48 × Turbidity + 21.21), with a coefficient of determination of $R^2 = 0.33$.*

Figure 4.1 shows a positive relationship between turbidity and measured TSS at Seemannshöft. Higher turbidity values generally corresponded to higher TSS concentrations, although the scatter around the fitted regression line was substantial. The fitted linear regression model was:

$$TSS = 0.48 \times \text{Turbidity} + 21.21$$

where TSS is expressed in mg/L and turbidity is expressed in FNU. The slope of 0.48 indicates that, within the matched dataset, each 1 FNU increase in turbidity was associated with an average increase of approximately 0.48 mg/L in TSS. The intercept of 21.21 mg/L represents the fitted baseline value when turbidity approaches zero and should be interpreted statistically rather than as a physical zero-turbidity condition. The model had a coefficient of determination of $R^2 = 0.33$ based on 118 matched observations.

The positive relationship shows that turbidity can be used as a local indicator of TSS variability at Seemannshöft. However, the R^2 value was moderate, so turbidity did not fully explain the measured TSS. Other factors, such as particle size, particle composition, organic matter content, and local hydrodynamic conditions, may also affect the turbidity–TSS relationship.

To further examine the variability in the turbidity–TSS relationship, three supplementary analyses were carried out. First, the matched measured turbidity and TSS observations were plotted as a time series. The two variables generally showed similar temporal behaviour, with several peaks occurring during the same periods. However, the magnitude of the response was not always proportional, indicating that turbidity can be used as an indicator of TSS variability but does not fully explain measured TSS.

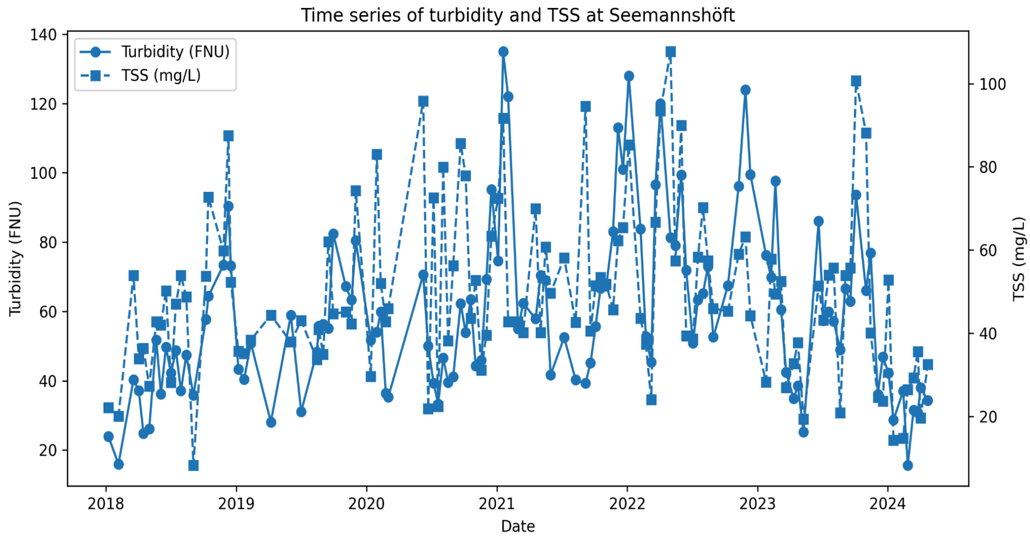

Figure 4.2. *Time series of matched measured turbidity and measured TSS observations at Seemannshöft. The two variables are shown using separate y-axes because they have different units. The comparison shows broadly similar temporal behaviour, although individual peaks do not always have the same magnitude.*

A log-transformed regression was also tested as a diagnostic check because the original scatter plot showed considerable spread, especially at higher values. The aim was to reduce the influence of high-value observations and to assess whether the turbidity–TSS relationship became more linear on a transformed scale. The log-log model was:

$$\log(TSS) = 0.65 \times \log(Turbidity) + 1.23$$

with an R^2 value of 0.30. This did not improve the fit compared with the original linear model, which had an R^2 of 0.33. Therefore, the original linear regression was retained for estimating TSS from the longer turbidity record.

The relationship was also tested separately for winter and summer. The winter subset showed a stronger relationship, with n = 32 and $R^2 = 0.50$, while the summer subset showed a weaker relationship, with n = 31 and $R^2 = 0.22$. This indicates that the turbidity–TSS relationship was seasonally variable. However, because the full matched dataset was limited, the annual regression was retained as a simple local screening relationship.

The regression was used to estimate TSS from the longer turbidity record. These estimated TSS values were then used in the temporal, distribution, hotspot, and environmental-driver analyses. Because the regression explained only part of the measured TSS variability, the estimated values were treated as indicative TSS-related values, not as exact replacements for direct TSS measurements.

4.2 Temporal variation of TSS

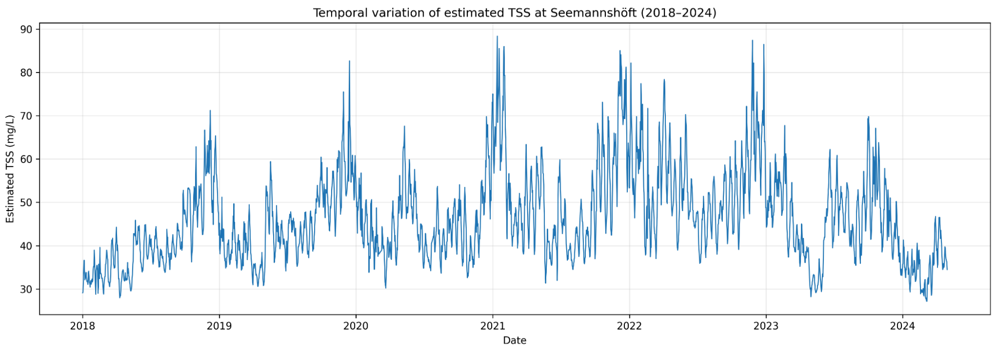

Figure 4.3. *Temporal variation of estimated total suspended solids (TSS) at Seemannshöft during 2018–2024. Estimated TSS values were derived from the site-specific turbidity–TSS regression shown in Figure 4.1 and should be interpreted as indicative TSS-related values rather than direct TSS measurements.*

Figure 4.3 shows the temporal variation of estimated TSS at Seemannshöft during 2018–2024. Most of the record shows moderate values, but shorter periods with elevated values are also visible. Several distinct peaks occurred during the study period, indicating that estimated TSS increased mainly during short events rather than following a smooth long-term trend.

From visual inspection of the time series, estimated TSS generally increased from 2018 towards 2022–2023, followed by lower values in 2024. The highest variability and several of the largest peaks occurred between 2021 and 2023, while 2024 showed fewer extreme peaks and a lower apparent baseline. Recent sediment-management reports for the Hamburg tidal Elbe provide useful context for this pattern, but these factors were not directly tested in this thesis (Hamburg Port Authority, 2024).

The study period also overlaps with the implementation phase of more stringent ballast water management requirements. However, these regulations concern ship ballast water discharge rather than direct local sediment concentrations. Therefore, they are treated here as operational background context, not as a direct explanation for the observed TSS trend.

Since the estimated TSS series was derived from turbidity, the values should be treated as indicative rather than direct TSS measurements. The time series was still useful for identifying elevated suspended-sediment periods and for the following distribution, hotspot, seasonal, and environmental-driver analyses.

4.3 Seasonal variability of estimated TSS

Monthly mean and median estimated TSS values were calculated for Seemannshöft for 2018–2024. This was done to examine seasonal variation and to check whether monthly averages were strongly influenced by short high-TSS peaks. The results are shown in Figure 4.4.

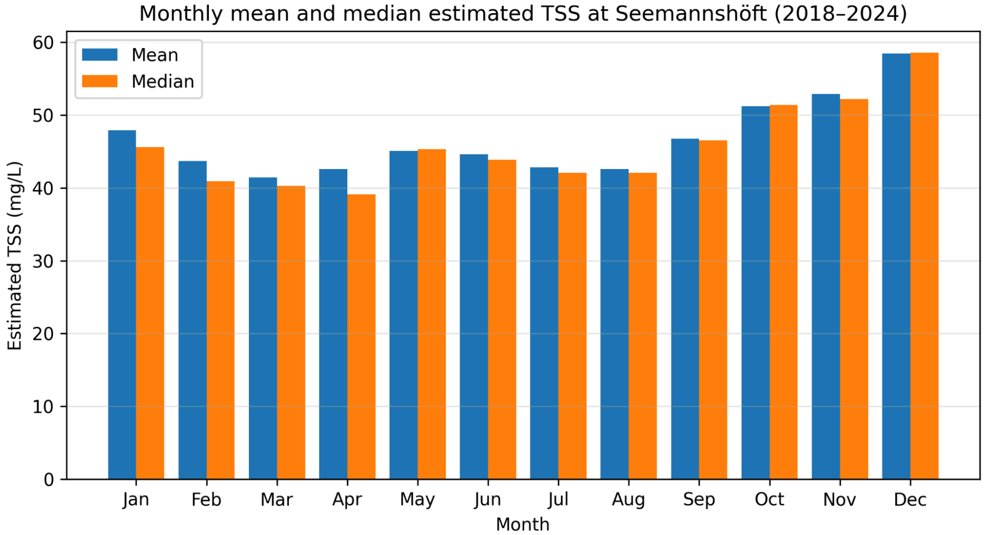

Figure 4.4. *Monthly mean and median estimated total suspended solids (TSS) at the Seemannshöft station during 2018–2024.*

Figure 4.4 shows the monthly mean and median estimated TSS at Seemannshöft during 2018–2024. The monthly mean values varied over the year, with lower values during spring and summer and higher values during autumn and early winter. The median values were also included because short high-TSS peaks can influence the mean more strongly than the median.

The comparison between mean and median shows a similar general seasonal pattern, although the mean is slightly higher than the median in some months. This indicates that occasional elevated events influenced the monthly averages, but did not fully control the seasonal pattern. October, November, and December still showed relatively high estimated TSS conditions, while spring and summer generally remained lower to moderate.

The monthly pattern therefore suggests that estimated TSS was not evenly distributed through the year. However, both monthly mean and median values can still hide short-term peaks. For this reason, seasonal differences were also examined using boxplots of estimated TSS grouped by season.

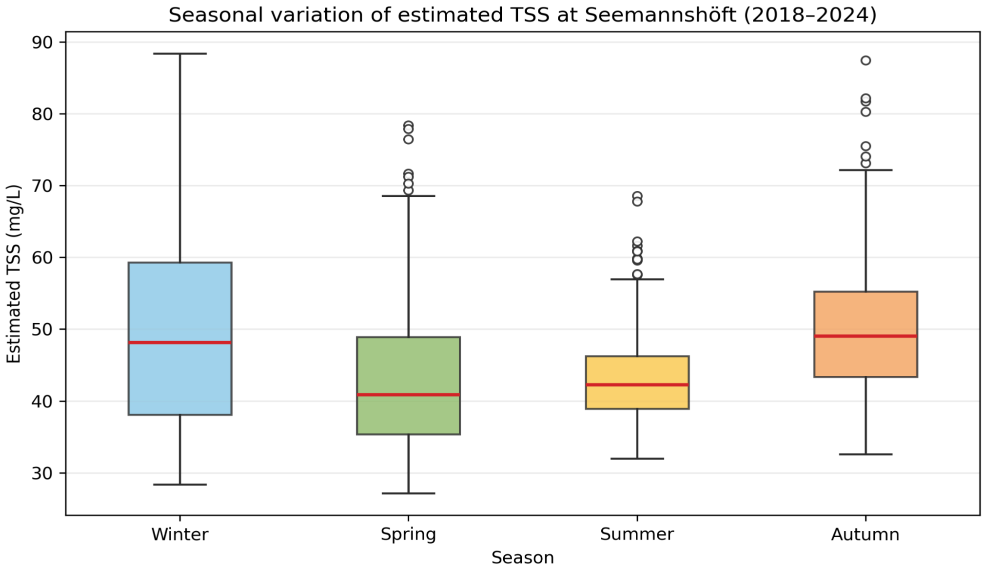

Figure 4.5*. Seasonal variation of estimated total suspended solids (TSS) at the Seemannshöft station during 2018–2024. The boxplots show the distribution of estimated TSS values across winter, spring, summer, and autumn.*

Figure 4.5 shows that the seasons differed not only in median values, but also in spread. Summer had the narrowest distribution, with relatively stable moderate TSS values. Spring was also mostly moderate, although some elevated observations were present.

Winter and autumn had higher median values and greater variability than spring and summer. Both seasons included a wider range of estimated TSS values and several elevated observations. Autumn was clearly higher than spring and summer, while winter also showed high values and a broad spread. Elevated suspended sediment conditions were therefore more common in the colder and transitional parts of the year.

The monthly and seasonal results show that TSS variability was not only related to average seasonal changes. The main seasonal difference was the wider spread and higher occurrence of elevated values in autumn and winter.

4.4 Distribution of estimated TSS

The frequency distribution of estimated TSS values at Seemannshöft for 2018–2024 was analysed. The result is shown in Figure 4.6.

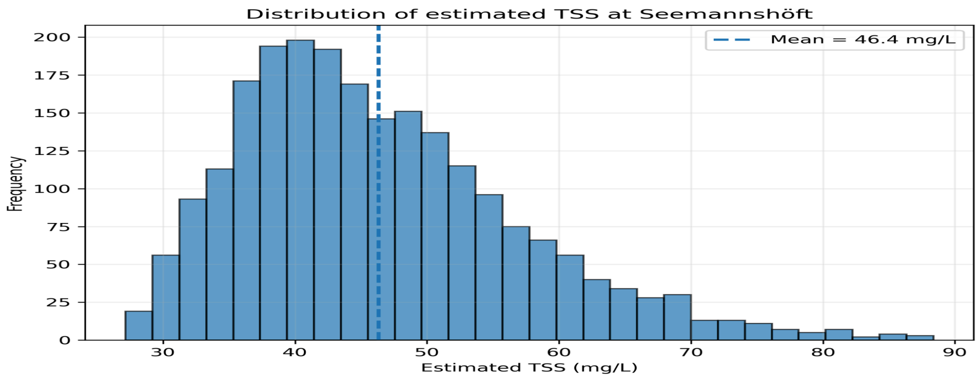

***Figure 4.6**. Distribution of estimated total suspended solids (TSS) at Seemannshöft during 2018–2024. The dashed line indicates the mean value of approximately 46.4 mg/L.*

Figure 4.6 shows that most estimated TSS values were concentrated within a moderate range, with the interquartile range extending from approximately 38.6 to 52.4 mg/L. The mean estimated TSS was 46.4 mg/L, while the median was slightly lower at 44.5 mg/L. This difference between the mean and median indicates that the distribution was positively skewed.

The distribution had a clear right-skewed pattern. Most observations were moderate, while a smaller number of elevated values formed the upper tail. Estimated TSS ranged from about 27.2 to 88.4 mg/L. This shows that high-concentration events occurred, but they made up only a small part of the full dataset.

The distribution shows that estimated TSS at Seemannshöft was mostly moderate. A small number of elevated observations formed the upper range of the dataset.

4.5 Identification of elevated estimated TSS events

The daily estimated TSS time series at Seemannshöft was examined using the 80 mg/L screening threshold defined in the Methods section. Elevated estimated TSS event days were defined as days when estimated TSS exceeded 80 mg/L. Their temporal distribution is shown in Figure 4.7.

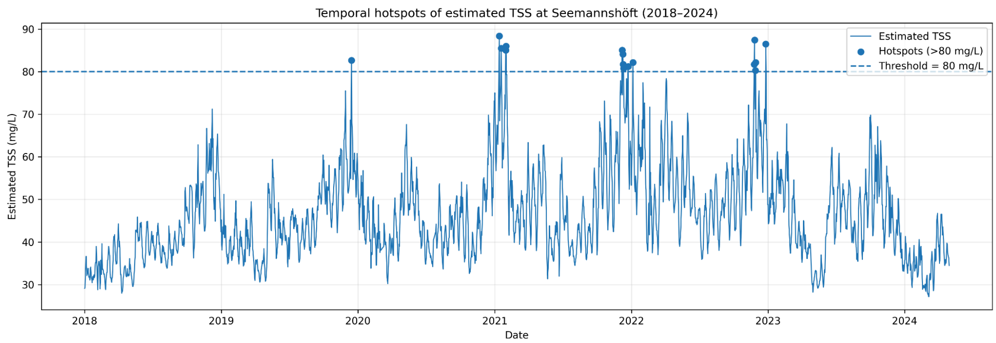

Figure 4.7. *Temporal distribution of elevated estimated total suspended solids (TSS) events at the Seemannshöft station during 2018–2024. Event observations indicate days on which estimated TSS exceeded the screening threshold of 80 mg/L. The dashed horizontal line marks the 80 mg/L screening threshold.*

Elevated estimated TSS event days were defined as days with estimated TSS above 80 mg/L. A total of 16 exceedance days were found out of 2244 daily values, equal to 0.71% of the record. The maximum estimated TSS was 88.37 mg/L on 13 January 2021. Most exceedance days occurred as short events rather than persistent periods.

Because the temporal exceedance analysis was based on estimated rather than directly measured TSS, the exceedance counts should be interpreted as screening-level indicators. Values close to the 80 mg/L threshold are especially uncertain because the turbidity–TSS regression explained only part of the measured TSS variability. Therefore, the hotspot results are used to identify potentially elevated suspended-sediment periods, not to define exact operational exceedance conditions.

To examine the sensitivity of hotspot identification to the selected screening threshold, exceedance counts were also calculated for 70 mg/L and 90 mg/L. This comparison was used to check whether the interpretation of high-TSS events as rare and episodic depended strongly on the 80 mg/L threshold.

Table 4.1. *Sensitivity of estimated TSS hotspot identification to different screening thresholds.*

Screening threshold (mg/L)	Number of exceedance days	Percentage of valid daily record (%)
70	76	3.39
80	16	0.71
90	0	0.00

The sensitivity check shows that the number of identified exceedance days increased when the threshold was lowered to 70 mg/L and decreased to zero when the threshold was raised to 90 mg/L. However, even under the lower 70 mg/L threshold, exceedance days represented only 3.39% of the valid daily record. This supports the interpretation that elevated estimated TSS conditions were episodic rather than persistent.

The hotspot observations were grouped within a small number of short event periods. They were not evenly distributed across the time series. Most hotspot events lasted only one day. A few lasted several days, including events in December 2021 and November 2022. The highest estimated TSS conditions therefore occurred as short episodes, not as persistent high background conditions.

Hotspot events were mainly observed between late 2019 and late 2022. Several occurred in winter or late autumn. This agrees with the seasonal analysis, where autumn and winter showed higher values and greater variability than spring and summer. However, because the number of hotspot observations was small, these events should be treated as exceptional high-TSS episodes, not as a continuous seasonal condition.

From an operational perspective, these short periods may be important because they indicate particle-rich conditions that could be relevant for ballast-water treatment screening and operational awareness.

4.6 Relationship between estimated TSS and environmental drivers

These analyses were exploratory and were used to assess whether simple environmental variables could explain turbidity variability; they were not intended to develop an operational forecasting model.

This section first presents pairwise comparisons between estimated TSS and individual environmental variables. It then presents river discharge as upstream hydrological context, followed by supplementary log-transformed turbidity models used to assess whether combined environmental variables and lagged information improved explanatory power.

The relationship between estimated TSS and selected environmental variables was examined at Seemannshöft. The variables were daily mean air temperature, daily mean wind speed, daily mean water level, electrical conductivity, and upstream river discharge at Neu Darchau. Air temperature, wind speed, and water level were compared directly with estimated TSS at Seemannshöft. Conductivity was used as a salinity-related proxy, while discharge was used as an upstream hydrological reference.

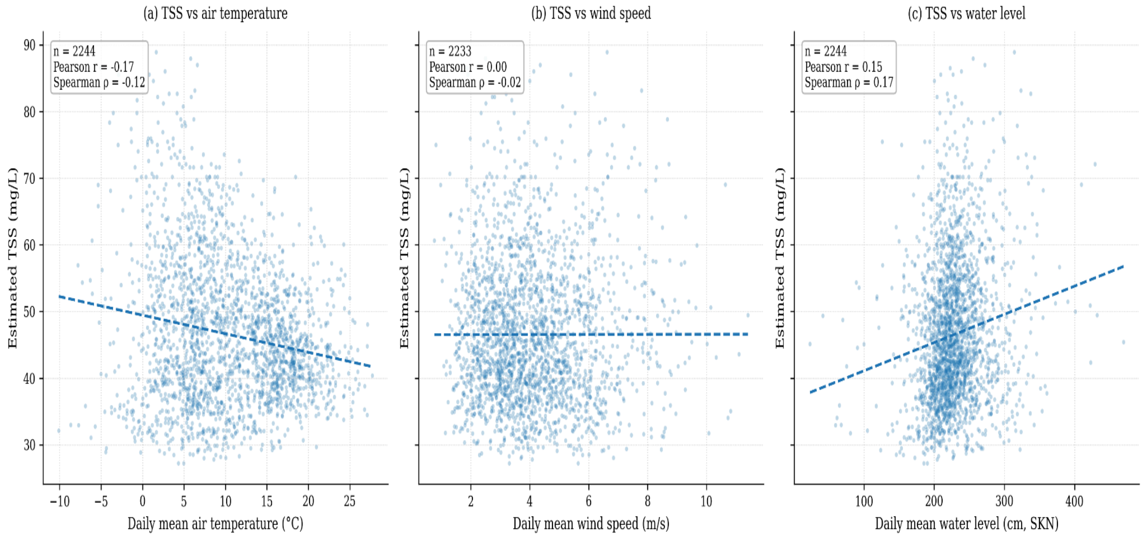

Figure 4.8. *Relationship between estimated total suspended solids (TSS) and environmental variables at Seemannshöft station. (a) TSS versus daily mean air temperature, (b) TSS versus daily mean wind speed, and (c) TSS versus daily mean water level. The fitted trend lines indicate generally weak relationships between TSS and the examined variables.*

Figure 4.8 shows a weak negative relationship between estimated TSS and daily mean air temperature. The regression line shows a slight decrease in TSS with increasing temperature, but the scatter is broad. The correlations were low: Pearson r = -0.17 and Spearman ρ = -0.12, with n = 2244. This indicates that air temperature was associated with only a small part of the observed TSS variability.

The relationship between estimated TSS and daily mean wind speed was also weak. The regression line was nearly flat, and the correlations were close to zero: Pearson r = 0.00 and Spearman ρ = -0.02, with n = 2233. The scatter plot does not show a consistent increase or decrease in TSS with stronger winds. At the daily scale used here, wind speed was not strongly associated with estimated TSS.

Daily mean water level showed a weak positive relationship with estimated TSS. The scatter plot shows a slight positive trend, with somewhat higher TSS values at higher water levels. However, the points are widely dispersed. The correlations were Pearson r = 0.15 and Spearman ρ = 0.17, with n = 2244. Daily mean water level alone therefore explained only a limited part of the estimated TSS variability.

Electrical conductivity at 25°C was also examined as a supplementary salinity-related proxy. This was done because salinity-related conditions may be relevant for estuarine mixing and suspended sediment dynamics. Direct station-based salinity data were not available consistently for the full study period.

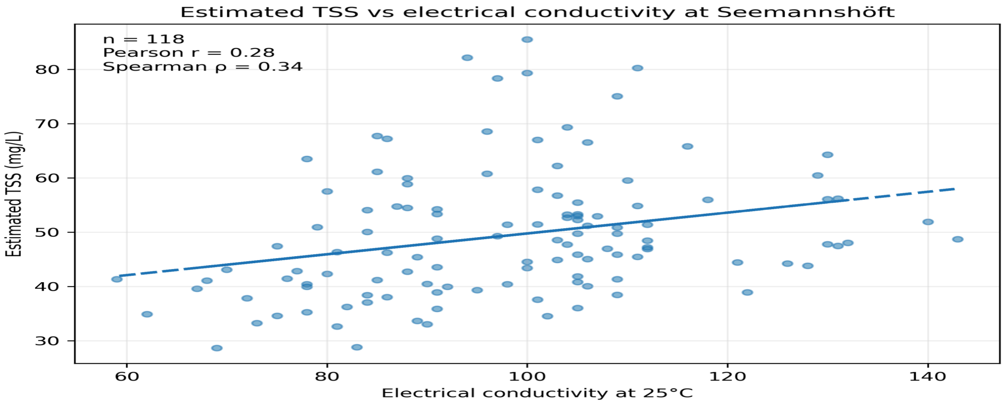

Figure 4.9. Relationship between estimated total suspended solids (TSS) and electrical conductivity at 25°C at Seemannshöft during 2018–2024. Electrical conductivity was used as a salinity-related proxy. The plot shows a weak-to-moderate positive relationship, with Pearson $r = 0.28$ and Spearman $\rho = 0.34$ based on 118 matched observations.

The conductivity comparison showed a weak-to-moderate positive relationship with estimated TSS. Pearson r was 0.28 and Spearman ρ was 0.34, based on 118 matched observations. Higher conductivity values were therefore associated with somewhat higher estimated TSS values. However, the number of matched observations was much smaller than for the other variables, and the scatter was still large. Conductivity should therefore be treated as supporting evidence, not as a direct controlling factor.

River discharge at Neu Darchau was included as an upstream hydrological reference for the broader Elbe River system. Because Neu Darchau is located upstream of the Port of Hamburg, the discharge record was not interpreted as a direct local predictor of estimated TSS at Seemannshöft. Instead, it was used to provide context for broader fluvial conditions during the study period.

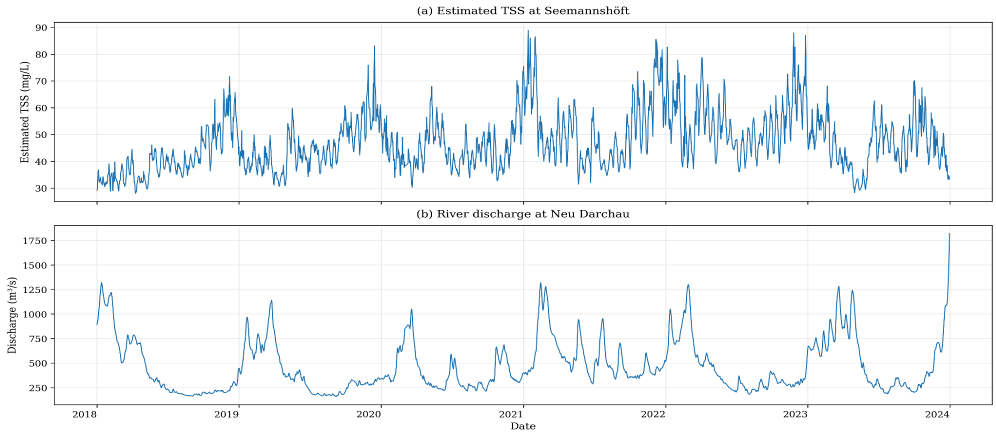

Figure 4.10. *Time series comparison between estimated total suspended solids (TSS) at Seemannshöft and river discharge at Neu Darchau during 2018–2024. Estimated TSS represents local suspended-sediment-related conditions at the main port station, while discharge at Neu Darchau is shown as an upstream hydrological reference for broader Elbe River conditions.*

The comparison shows that estimated TSS at Seemannshöft did not follow a simple one-to-one pattern with upstream discharge. High discharge at Neu Darchau did not always coincide with the highest estimated TSS values. Several elevated TSS periods also occurred during moderate discharge conditions.

Because estimated TSS was derived from measured turbidity, measured turbidity was also used in supplementary log-transformed analyses to test whether the environmental variables explained the original turbidity signal more clearly. A multiple linear regression model was fitted using log-transformed measured turbidity as the response variable and daily mean air temperature, wind speed, water level, and Neu Darchau discharge as predictors.

The model explained more variability than the individual pairwise relationships, with $R^2 = 0.294$ and an adjusted $R^2 = 0.292$ based on 2113 matched observations. In the standardized model, discharge and air temperature showed the strongest negative associations with log-transformed turbidity, while water level showed a positive association and wind speed had only a weak negative association.

The correlation matrix of the variables used in the log-transformed turbidity model is shown in Figure 4.10. This provides an overview of the pairwise associations among the model variables and helps interpret the multivariable regression results.

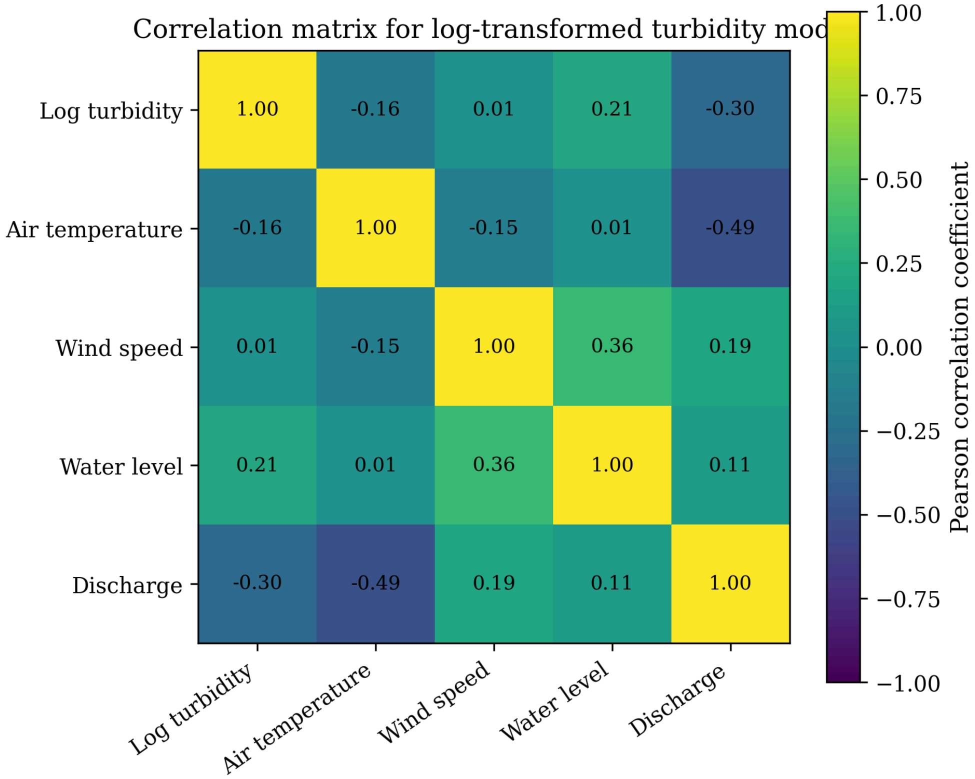

Figure 4.11. *Pearson correlation matrix for the variables used in the log-transformed turbidity model. Values indicate pairwise Pearson correlation coefficients between log-transformed turbidity and the environmental predictors.*

The matrix shows that log-transformed turbidity had weak correlations with the individual environmental variables, including a weak negative correlation with discharge and a weak positive correlation with water level. It also shows that some predictors were correlated with each other, especially air temperature and discharge. This supports the use of the multivariable model as a sensitivity check, while also showing that the available environmental variables do not fully explain turbidity variability.

To further examine the relative importance of the environmental variables, an exploratory Random Forest regression was applied using log-transformed measured turbidity as the response variable. This analysis was used to identify which predictors contributed most to the non-linear model, rather than to develop an operational prediction model.

The Random Forest model gave a test R^2 of 0.377 for one train-test split, but cross-validation performance was unstable. Therefore, the feature importance results were interpreted only as an exploratory indication of relative variable importance.The Random Forest model was fitted using the original predictor values without standardization.

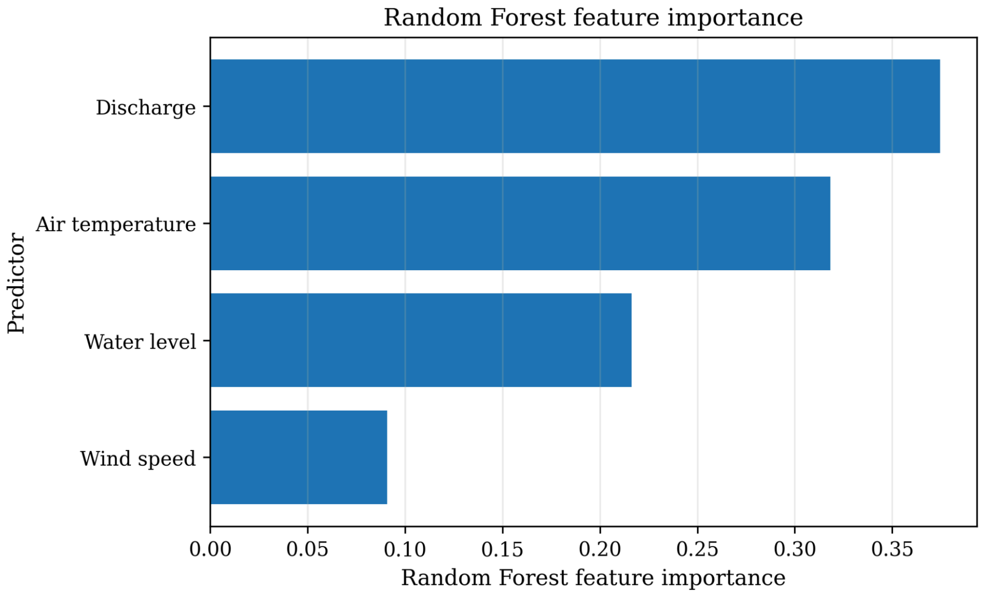

Figure 4.12. *Random Forest feature importance for the exploratory log-transformed turbidity model. The model used daily mean air temperature, wind speed, water level, and Neu Darchau discharge as predictors. Higher feature importance values indicate a larger relative contribution to the model.*

The Random Forest feature importance results indicate that discharge and air temperature contributed most to the model, followed by water level, while wind speed had the lowest relative importance. The Random Forest model was fitted using the original predictor values without standardization. The result is broadly consistent with the standardized multiple regression, where discharge and air temperature also showed the strongest associations with log-transformed turbidity.

However, the Random Forest model was interpreted as exploratory because cross-validation performance was unstable. The result should therefore be used to support interpretation of relative driver importance rather than as a reliable predictive model.

Lagged correlations were tested for lag times from 0 to 7 days. The strongest lagged association was found for discharge at a 7-day lag, but the relationship remained weak-to-moderate (Pearson $r = -0.34$). Water level showed its strongest association with same-day turbidity (Pearson $r = 0.21$), while wind speed showed almost no lagged relationship. These results indicate that lagged environmental variables did not substantially improve the explanation of log-transformed turbidity. The full lagged-correlation comparison is shown in Figure B2 in Appendix B.

Daily rainfall was also tested as an additional environmental predictor using Open-Meteo historical precipitation data for the study location. Same-day rainfall and rainfall lags from 1 to 7 days were examined. Rainfall showed only very weak positive correlations with log-transformed turbidity, with the strongest correlations for same-day and one-day lagged rainfall. Adding rainfall lag variables to the prediction models did not improve model performance. Therefore, rainfall was treated as a supplementary check and was not retained as a major explanatory variable in the final interpretation.

A time-ordered prediction test was then performed to examine whether log-transformed turbidity could be predicted when lagged variables were included. The models were trained on 2018–2022 data and tested on 2023. The prediction results showed a clear difference between environmental-driver prediction and persistence-based prediction. Models using only environmental variables had limited predictive skill, indicating that temperature, wind speed, water level, and discharge alone were not sufficient to explain short-term turbidity variability.

When lagged turbidity was included, model performance improved strongly. Linear Regression achieved the highest test performance ($R^2 = 0.924$), followed by XGBoost ($R^2 = 0.914$) and Random Forest ($R^2 = 0.900$), while ARIMA(1,0,0) performed poorly for the same test period. This indicates that turbidity was strongly predictable when previous turbidity observations were available, but not from environmental variables alone.

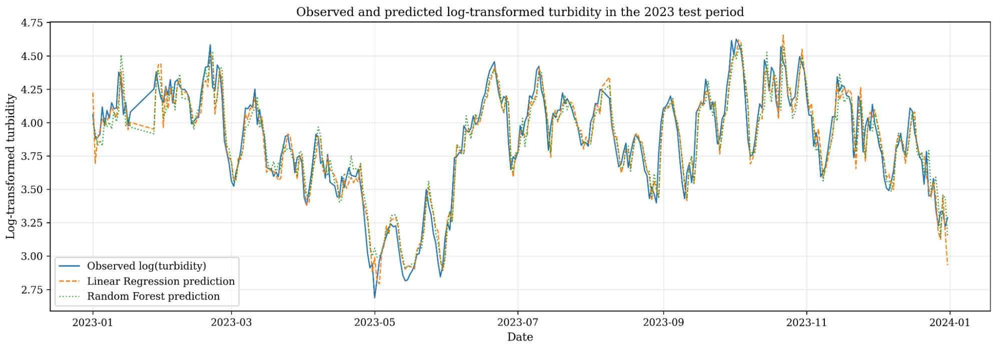

Figure 4.13. *Observed and predicted log-transformed turbidity during the 2023 test period using time-ordered prediction models with lagged variables. The models were trained on 2018–2022 data and tested on 2023. The close agreement mainly reflects the strong influence of one-day lagged turbidity rather than environmental variables alone.*

The lagged prediction models followed the observed turbidity pattern closely during the 2023 test period. This indicates that short-term turbidity prediction was mainly driven by persistence in the turbidity time series rather than by the environmental variables alone.

A supplementary Random Forest forecast-window check was also carried out to clarify the model setup and test how much past information was useful for short-term prediction. The model used past values of log-transformed turbidity, air temperature, wind speed, water level, discharge, and rainfall as input variables.

Three input windows were tested, using the previous 7, 14, and 21 days, and the model was used to predict log-transformed turbidity 1, 2, and 3 days ahead. The data were split chronologically, with 2018–2021 used for training, 2022 for validation, and 2023 as an independent test period. The best validation performance was obtained for the 21-day input window with a 1-day forecast horizon, while the 14-day window gave a similar and slightly higher test performance in 2023.

Overall, the model performed best for 1-day prediction, and performance decreased for 2- and 3-day horizons. This supports the interpretation that turbidity predictability was mainly short-term and persistence-driven. The full forecast-window comparison is provided in Appendix B.

In contrast, the +7 days prediction test showed substantially lower performance. Persistence-only models achieved R^2 values of 0.02–0.25, while models including environmental variables increased to R^2 values of 0.36–0.41. These results support the interpretation that short-term prediction was mainly driven by temporal persistence in turbidity, while environmental variables provided additional but secondary information.

As an additional exploratory check, PCA was applied to the standardized environmental variables. The first two principal components explained about 72% of the total environmental-variable variance, with PC1 explaining 41.7% and PC2 explaining 30.3%. PC1 mainly represented a contrast between higher discharge, wind speed, and water level versus lower air temperature, while PC2 was mainly related to water level, air temperature, and wind speed, with discharge contributing in the opposite direction.

However, PC1 and PC2 showed only weak correlations with log-transformed turbidity. Although PC4 showed a stronger negative correlation with log-transformed turbidity, it explained only 12.2% of the environmental-variable variance. Therefore, the PCA supported the interpretation that the dominant environmental-variable structure did not strongly explain turbidity variability. The PCA explained-variance and loading tables are provided in Appendix B as supplementary numerical detail.

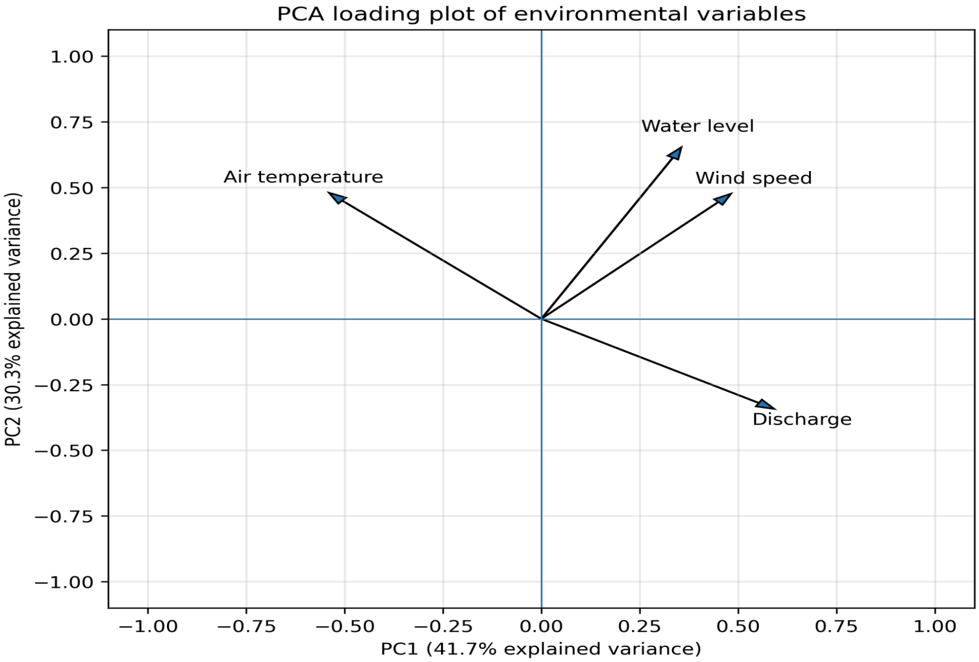

Figure 4.14. *PCA loading plot of standardized environmental variables used in the exploratory turbidity analysis. Turbidity and estimated TSS were not included as PCA input variables; the PCA was used to summarize the covariance structure among the environmental variables. The arrows show the direction and contribution of each variable in the first two principal components. PC1 explained 41.7% of the variance and PC2 explained 30.3%.*

Figure 4.14 shows that wind speed and water level point in a similar direction, indicating that they contributed in a broadly similar way to the first two principal components. Discharge and air temperature point in opposite directions, suggesting contrasting seasonal or hydrological patterns. Together, PC1 and PC2 explained 72.0% of the total environmental-variable variance, but these components were only weakly related to log-transformed turbidity. This supports the interpretation that the main structure in the environmental variables did not strongly explain turbidity variability at Seemannshöft.

Overall, the results indicate that the examined environmental drivers had limited explanatory value for estimated TSS and turbidity variability at Seemannshöft. Air temperature showed a weak negative relationship with estimated TSS, wind speed showed virtually no relationship, water level showed only a weak positive association, and conductivity provided supplementary evidence of salinity-related mixing effects. Upstream discharge at Neu Darchau provided useful hydrological context, but did not explain local variability in a simple direct manner.

The multiple regression, Random Forest, lagged-correlation analysis, PCA, and time-ordered prediction tests all support the same interpretation: the available environmental variables provided useful context, but did not fully explain short-term turbidity variability. Suspended sediment dynamics at the study site were therefore likely influenced by more complex and episodic processes, such as tidal dynamics, salinity-related mixing, short-term resuspension events, shipping activity, dredging-related disturbance, or changes in upstream sediment supply.

4.7 Comparison of satellite-derived NDTI with in-situ turbidity and TSS at Seemannshöft

Satellite-derived optical information was also examined. The aim was to check whether remotely sensed surface conditions were consistent with station-based turbidity and TSS observations. Sentinel-2 derived NDTI values were extracted for the Seemannshöft water-only polygon for 2018–2024. A 40% cloud threshold was used, which resulted in 273 valid satellite observations. These observations were compared with available in-situ turbidity and TSS/filter residue data from the FGG Elbe data portal using exact-date matching.

The NDTI–turbidity comparison gave 239 matched observations (Figure 4.15). The relationship was weakly positive, with Pearson r = 0.18 and Spearman ρ = 0.22. Higher turbidity values were generally linked to slightly higher NDTI values, but the scatter was large. NDTI alone was therefore not a strong quantitative predictor of station-based turbidity at Seemannshöft. Still, the positive trend shows that NDTI can provide supporting information on relative surface turbidity.

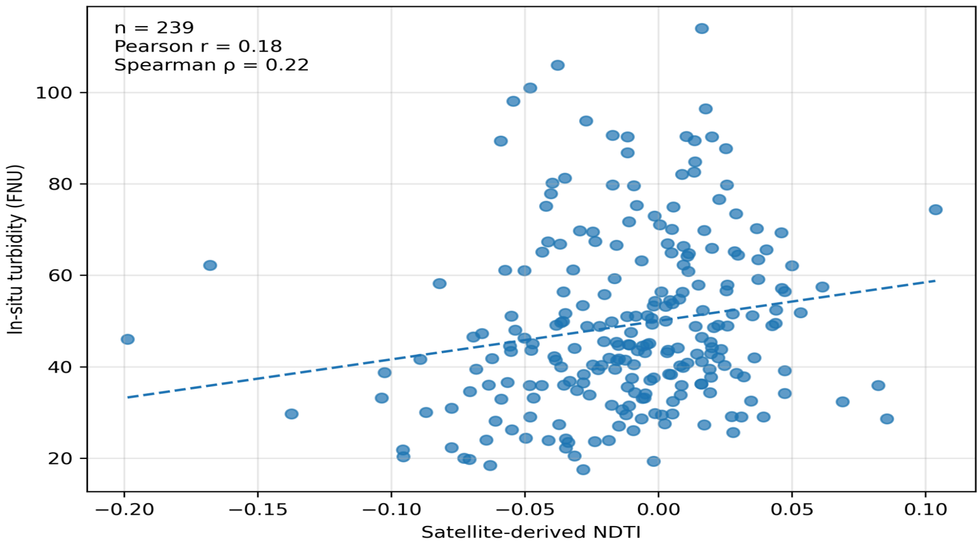

Figure 4.15. *Relationship between satellite-derived NDTI and in-situ turbidity at Seemannshöft based on exact-date matching during 2018–2024 (n = 239). The dashed line indicates the linear trend. The relationship was positive but weak (Pearson r = 0.18; Spearman ρ = 0.22).*

The NDTI–TSS/filter residue comparison was more limited by temporal overlap. Although the satellite dataset covered 2018–2024 and the cloud threshold was increased to 40%, only 15 exact-date matches were obtained (Figure 4.16). These observations showed a weak-to-moderate positive tendency, with Pearson r = 0.30 and Spearman ρ = 0.40. However, the sample size was small. Therefore, this relationship should be interpreted cautiously and not as a robust predictive relationship.

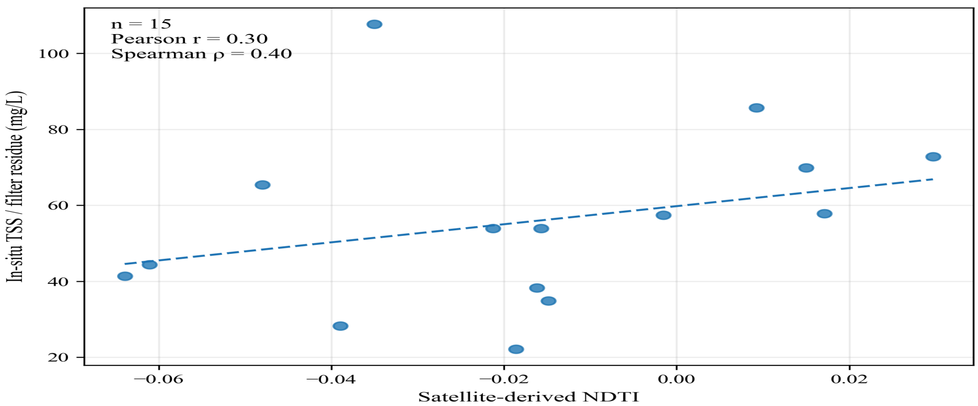

Figure 4.16. *Relationship between satellite-derived NDTI and in-situ TSS/filter residue at Seemannshöft based on exact-date matching during 2018–2024 (n = 15). The dashed line indicates the linear trend. The relationship shows a weak to moderate positive tendency, but the small sample size limits robust interpretation.*

The satellite comparison shows that NDTI is better used as a complementary optical indicator than as a direct replacement for measured TSS or turbidity measurements. The NDTI–turbidity comparison had more matched observations and gave a better basis for assessing relative optical variability. The NDTI–TSS comparison was limited by the small number of exact-date matches between satellite overpasses and TSS sampling.

4.8 Spatial hotspot frequency of satellite-derived NDTI

The spatial distribution of satellite-derived NDTI was examined across the Port of Hamburg using valid Sentinel-2 observations from 2018–2024. To assess recurring spatial patterns, a multi-year hotspot-frequency approach was used to identify areas where elevated optical turbidity signals occurred repeatedly.

After cloud filtering and water masking, 273 valid Sentinel-2 observations were retained. The port-scale P90 and P95 NDTI thresholds were 0.00455 and 0.01636, respectively. For the spatial hotspot-frequency analysis, the stricter P95 threshold was used. Each valid Sentinel-2 observation was classified pixel by pixel, and pixels with NDTI values above the P95 threshold were treated as high-NDTI observations. Pixels with fewer than 20 valid observations during the study period were excluded, and a 150 m focal mean was applied to reduce pixel-level speckle.

Figure 4.15 shows the resulting smoothed P95 NDTI hotspot-frequency map. Hotspot frequency represents the percentage of valid Sentinel-2 observations in which each pixel exceeded the port-scale P95 NDTI threshold. The map therefore shows where elevated optical turbidity signals occurred repeatedly during 2018–2024, rather than representing a single satellite event.

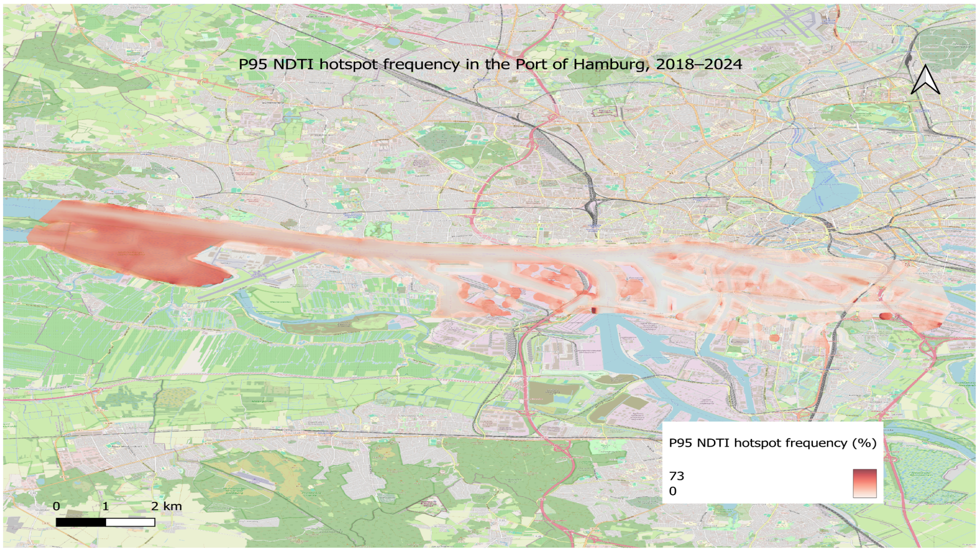

Figure 4.17. *Smoothed P95 NDTI hotspot frequency in the Port of Hamburg during 2018–2024. Hotspot frequency represents the percentage of valid Sentinel-2 observations exceeding the port-scale P95 NDTI threshold of 0.0163. The term hotspot is used here in a spatial sense and refers to pixels with recurring high relative NDTI values. Pixels with fewer than 20 valid observations were excluded, and a 150 m focal mean was applied to reduce pixel-level speckle. The mapped area includes the approximate main harbour area shown in Figure 3.1b, but the map provides spatial screening information only and does not indicate observed ballast-water uptake or discharge locations. Identifying actual ballast-water operation locations would require operational data such as ballast-water records, port-call information, berth data, or AIS-based vessel-activity analysis.*

The smoothed P95 hotspot-frequency map shows that recurring elevated optical turbidity conditions were spatially heterogeneous across the study area. Higher hotspot frequencies appeared in parts of the western main Elbe reach as well as in several inner-port and harbour-basin areas, while lower-frequency zones occurred along parts of the central channel. The smoothed P95 hotspot frequency ranged from 0% to 73.0%, with a mean value of 15.9% across valid pixels.

These findings indicate that elevated surface turbidity signals were not uniformly distributed across the Port of Hamburg. However, the hotspot-frequency map should be interpreted as a relative optical screening product rather than a direct TSS exceedance map. It provides spatial context for identifying areas with recurring elevated optical turbidity signals, but local in-situ measurements remain necessary for interpreting actual suspended sediment concentrations.

4.9 Temporal distribution of matched NDTI–TSS observations

The monthly and seasonal distribution of the 15 exact-date NDTI–TSS matches was examined. This was done to check how representative the limited matched dataset was over time (Figure 4.18).

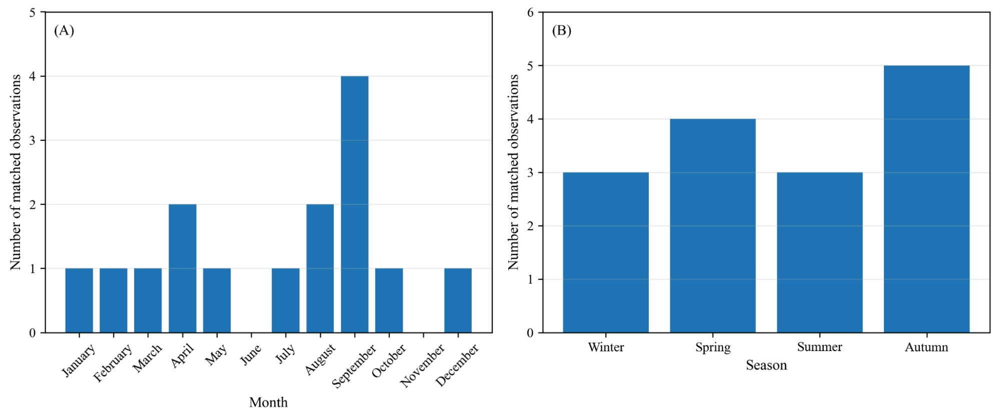

Figure 4.18. *Monthly (a) and seasonal (b) distribution of exact-date matched NDTI–TSS observations at Seemannshöft during 2018–2024 (n = 15). The matched observations were distributed across all seasons, although monthly coverage remained sparse and uneven.*

The matched observations were distributed across all four seasons. There were three observations in winter, four in spring, three in summer, and five in autumn. Therefore, the matched dataset was not limited to one season. Monthly coverage was available for most months, but it was uneven. September had the highest number of matches, with four observations. Several months had only one or two matches, and no matched observations were available in June or November.

The matched NDTI–TSS observations covered all seasons, but the dataset was still sparse for the full 2018–2024 period. It can support a cautious comparison between NDTI and measured TSS. However, it is not sufficient for strong seasonal interpretation or robust predictive modelling.

The limited and uneven temporal distribution of matched NDTI–TSS observations reduced the robustness of the satellite–TSS comparison. Therefore, Sentinel-2 NDTI was interpreted as a relative optical turbidity indicator rather than as a validated satellite-derived TSS estimate.

Discussion

Before discussing the interpretation and limitations of the results, Table 5.1 summarizes how the main objectives of the thesis were addressed by the analyses. This provides an overview of the link between the goal document, the applied methods, and the main thesis outputs.

Table 5.1. *Alignment between thesis objectives, analytical outputs, and thesis sections.*

Thesis objective / element	Analytical output	Main section(s)
Assess turbidity- and TSS-related conditions	Local turbidity–TSS relationship; estimated daily TSS	4.1–4.2
Identify temporal, seasonal, and elevated events	Monthly/seasonal patterns; TSS distribution; 80 mg/L hotspot screening	4.3–4.5
Examine environmental drivers	Pairwise comparisons; conductivity; discharge context; regression, RF, and lagged prediction tests	4.6
Compare satellite optical information with in-situ data	Sentinel-2 NDTI compared with measured turbidity and TSS/filter residue	4.7
Assess spatial turbidity-related patterns	P95 NDTI hotspot-frequency map from valid Sentinel-2 observations	4.8
Consider local port-related processes	Qualitative interpretation of navigation, dredging, and local resuspension limitations	5.4–5.6
Link findings to ballast-water relevance	Field-visit context; filtration/UV relevance; practical screening framework	3.2.8, 5.4, 5.7

The table shows that the thesis addresses the goal document through an observational and screening-based approach. Some elements, such as temporal hotspot identification and satellite-based spatial screening, were analysed quantitatively. Other elements, especially ship-induced sediment resuspension and operational BWMS implications, were treated qualitatively because the required high-resolution operational and system-specific datasets were not available.

5.1 Reliability and limitations of satellite-derived NDTI

Satellite-derived NDTI was useful for interpreting surface turbidity conditions in the Hamburg Port area. The comparison with monitoring station observations showed that NDTI captured part of the temporal variability in suspended-sediment-related optical conditions. This means that Sentinel-2 imagery can help identify relative changes in turbidity. However, NDTI should not be treated as a direct measurement of TSS.

Several limitations should be considered when using NDTI in this study area. NDTI is an optical surface indicator. It is affected by atmospheric conditions, cloud cover, sun glint, water masking, and the timing of satellite overpasses. Because of this, not all in-situ observations could be matched with valid satellite observations. The satellite–in-situ comparison was therefore limited by temporal overlap.

The Port of Hamburg is also a narrow and complex estuarine-port environment. Mixed pixels, shoreline effects, vessels, harbour infrastructure, and shallow or highly reflective surfaces may affect the satellite signal. This is especially important in narrow channels and near port structures, where one satellite pixel may not represent only open water.

In the spatial analysis, NDTI was used to produce a multi-year hotspot-frequency map rather than a direct TSS map. This strengthens the spatial interpretation of the satellite results because the analysis is based on all valid Sentinel-2 observations from 2018–2024 and identifies areas where elevated NDTI occurred repeatedly. The P95 hotspot-frequency map therefore provides screening-level information on recurring elevated optical turbidity signals across the port area.

However, the spatial hotspot-frequency map should still be interpreted with caution. The mapped hotspots represent relative optical turbidity responses, not direct TSS exceedance areas or measured suspended-sediment concentrations.

Higher NDTI values may indicate more turbid surface water, but the index does not directly account for particle size, sediment composition, coloured dissolved organic matter, water depth, or vertical mixing. In addition, mixed pixels, shoreline effects, vessels, harbour infrastructure, atmospheric conditions, cloud filtering, and sun-glint effects may influence the satellite signal.

For this reason, Sentinel-2-derived NDTI was used as supporting spatial information rather than as a stand-alone quantitative method. The hotspot-frequency map can help identify areas where elevated optical turbidity signals occur more frequently, but local station-based turbidity and TSS measurements remain necessary for interpreting actual suspended-sediment conditions and for any operational assessment related to ballast water treatment.

5.2 Temporal and seasonal variability of TSS

The temporal analysis showed that estimated TSS at Seemannshöft was not constant during 2018–2024. Most values were moderate, but several short periods had clearly higher values. This pattern suggests that short-term events were important for TSS variability.

The difference between the daily time series and the monthly means is important. The daily record showed several clear peaks. The monthly means were smoother and mainly showed lower values in spring and summer and higher values in autumn and early winter. This shows that monthly averages can hide short high-TSS events.

Seasonal variability was clearer in the spread of the data than in the average values alone. Summer had a narrow distribution and mostly moderate TSS values. Autumn and winter had higher medians, wider ranges, and more elevated observations. This suggests that high-TSS events were more common during these seasons.

Therefore, the main seasonal signal was not a simple smooth increase or decrease through the year. It was mainly the higher occurrence of elevated values in autumn and winter.

5.3 Distribution patterns and exceedance behaviour of estimated TSS

The distribution and hotspot analyses together suggest that suspended sediment conditions at Seemannshöft were characterised less by persistently high background concentrations and more by a combination of moderate baseline conditions and occasional elevated episodes.

Most estimated TSS values were concentrated within a moderate range, with a mean of approximately 46.4 mg/L and a median of approximately 44.5 mg/L. At the same time, the right-skewed distribution and the presence of upper-tail values indicate that a smaller number of elevated observations contributed disproportionately to the overall variability.

This interpretation is reinforced by the hotspot analysis, which showed that values above the selected threshold were rare and temporally clustered rather than evenly distributed across the record. Only 16 observations exceeded the 80 mg/L hotspot threshold, corresponding to 0.71% of the daily record.

The threshold-sensitivity check further supports this interpretation: lowering the screening threshold to 70 mg/L increased the number of exceedance days to 76, but this still represented only 3.39% of the valid daily record, while no days exceeded 90 mg/L.

These hotspot observations occurred within a limited number of short event periods, mainly between late 2019 and late 2022, with the maximum estimated TSS value of 88.37 mg/L occurring on 13 January 2021. This suggests that the most elevated suspended sediment conditions did not arise as a persistent background state, but as temporally concentrated episodes.

From an operational perspective, this distinction is important. Ballast water treatment systems are unlikely to be challenged primarily by moderate background conditions, but rather by short-lived periods in which suspended matter increases sharply.

The fact that high-TSS events were clustered rather than continuously distributed implies that operational risk may be concentrated within specific windows of time. This makes the identification of elevated episodes particularly relevant when assessing challenging water quality in a port environment.

Taken together, the distribution and hotspot results show that the upper range of estimated TSS was shaped by a small number of elevated events. This supports the interpretation that the most challenging suspended sediment conditions were episodic rather than representative of the general background state.

5.4 Interpreting the drivers of TSS variability

The results show that no single environmental variable explained estimated TSS variability well at Seemannshöft. Daily mean wind speed had almost no relationship with estimated TSS. Air temperature showed only a weak negative relationship, while daily mean water level showed a weak positive relationship. Electrical conductivity showed the clearest positive association with estimated TSS, but this comparison was based on fewer matched observations. For this reason, conductivity should be treated as supplementary evidence of salinity-related conditions rather than as a direct controlling factor.

River discharge at Neu Darchau provided useful upstream hydrological context for the broader Elbe River system. However, it did not show a simple one-to-one relationship with local estimated TSS at Seemannshöft. Periods of higher discharge did not always match the highest estimated TSS values, and elevated TSS also occurred during more moderate discharge conditions. This suggests that upstream discharge may influence the broader hydrological and sediment setting, but it does not directly explain local TSS variability in the Port of Hamburg.

The log-transformed multivariable regression provided a useful sensitivity check. It explained a larger share of turbidity variability than the individual pairwise comparisons, but the explanatory power remained moderate. This supports the interpretation that the selected daily environmental variables provide useful context, but do not fully explain turbidity and TSS variability in the port area.

The weak relationships with the tested variables show that simple atmospheric or hydrological indicators were not enough to explain the timing and magnitude of TSS variability. In estuarine systems, suspended sediment variability is often shaped by the interaction of river discharge, tidal forcing, local resuspension, sediment availability, salinity-related mixing, and transport processes, rather than by one driver alone (Chen et al., 2015; Liu et al., 2023; Wan & Wang, 2018).

Recent sediment-management information provides additional context for the lower estimated TSS values observed in 2024. The 2024 water-depth maintenance report states that around 3.07 million tonnes of dry matter sediment were dredged in Hamburg in 2024, about 1.2 million tonnes less than in the previous year. The report links the lower maintenance demand to improved hydrological conditions, increased export of excess fine sediment, and minimized maintenance dredging (Hamburg Port Authority, 2024).

These observations are consistent with the lower estimated TSS values in 2024, but they should be interpreted as contextual information rather than direct evidence of causality, because dredging records and sediment-management measures were not included as quantitative drivers in this thesis.

The Random Forest feature-importance analysis provided an additional exploratory check of the relative role of the environmental variables. Discharge and air temperature had the highest relative importance among the available environmental predictors, followed by water level, while wind speed had the lowest importance. However, the unstable cross-validation performance shows that this result should not be interpreted as a robust predictive explanation of short-term turbidity variability.

The time-ordered prediction test provided an important distinction between environmental predictability and temporal persistence. Models using lagged turbidity performed much better than models using only environmental variables. Linear Regression, XGBoost, and Random Forest all predicted the 2023 test period well, while ARIMA(1,0,0) performed poorly in this setup.

The high performance of the lagged models mainly reflects strong temporal persistence in turbidity, because previous turbidity observations dominated the prediction. This suggests that turbidity can be predicted well in the short term when recent turbidity measurements are available, but the available environmental variables alone do not fully explain the underlying drivers of variability.

The lag analysis further supports this interpretation. Although discharge showed a slightly stronger association at longer lags, the correlations remained limited. Water level showed its strongest association with same-day turbidity, while wind speed showed almost no lagged relationship. These results suggest that daily environmental variables and their short lags are useful for screening and interpretation, but are not sufficient on their own to explain short-term turbidity peaks.

The multi-year P95 NDTI hotspot-frequency map also showed that turbidity-related optical conditions were not spatially uniform across the Port of Hamburg. Recurring elevated NDTI conditions occurred unevenly across the mapped port area, indicating spatial heterogeneity in surface optical turbidity signals. These zones should be interpreted as relative optical turbidity hotspots, not as direct measurements of TSS concentration or TSS exceedance areas.

This spatial pattern supports the interpretation that local morphology, estuarine hydrodynamics, salinity gradients, and port-related processes may jointly influence suspended-sediment-related conditions. This is consistent with studies of estuarine turbidity maxima, where hydrodynamics, salinity gradients, and morphology jointly influence sediment concentration and trapping in tidal systems (Hesse, Zorndt, & Fröhle, 2019; Torres-Bejarano et al., 2025).

One local process that could not be tested quantitatively in this study is ship-induced sediment resuspension. In harbour basins and navigation channels, propeller wash, vessel manoeuvring, berth operations, and ship traffic may locally resuspend bed material and increase turbidity over short time scales.

Such processes are potentially relevant in a port setting such as Hamburg, especially because the statistical analysis showed that the available daily environmental variables did not fully explain turbidity variability. However, this thesis did not include AIS data, vessel movement records, propeller characteristics, berth-scale operation data, dredging-operation records, or high-frequency turbidity observations close to ship manoeuvring areas. Therefore, ship-induced resuspension could only be considered qualitatively as a possible local contributor, not as a quantified driver of the observed TSS or turbidity variability.

The field visit provided additional operational context. The discussion during the visit indicated that particle-rich water conditions, including high TSS and particle characteristics, may be more relevant for treatment challenges than turbidity alone. This is especially important for filtration and UV-based treatment stages.

These observations were qualitative and vessel-specific. Still, they help explain why episodic high-TSS periods may be operationally relevant. This is also consistent with industry reporting on challenging water quality, where BWMS challenges are described as practical operational issues in ports worldwide, including Hamburg (INTERTANKO, 2026).

Together, the results suggest that TSS variability in the study area was influenced more by short-term and interacting estuarine and port-related processes than by steady environmental conditions. This helps explain why wind speed, air temperature, water level, and upstream discharge had limited explanatory power when considered separately. It is also consistent with the temporal, seasonal, hotspot, conductivity, satellite, and field-visit analyses, which showed episodic, spatially variable, and operationally relevant suspended-sediment-related conditions.

5.5 Comparison with previous studies

The temporal, seasonal, and hotspot patterns found in this study are consistent with previous studies showing that suspended-sediment conditions in estuaries are often event-driven rather than smoothly seasonal (Wan & Wang, 2018; Zhu et al., 2021).

In this study, seasonal differences were mainly expressed through the spread of estimated TSS values and the occurrence of elevated events, especially during autumn and winter, rather than through average conditions alone. The hotspot analysis also showed that exceedances above the selected threshold were rare and temporally concentrated, indicating that challenging water-quality conditions were mainly linked to short events.

The satellite-based results are also consistent with previous remote-sensing studies showing that optical indicators can capture broad suspended-sediment-related patterns in estuarine waters, but cannot replace measured concentrations (Chowdhury et al., 2023). In this study, Sentinel-2-derived NDTI helped visualize relative spatial variability and possible hotspot areas within the port. However, these areas should be interpreted as relative high-NDTI zones, not as direct high-TSS zones.

Local context is important when comparing these results with previous studies. The Port of Hamburg is a complex estuarine-port setting, where water quality may reflect both wider river-estuary conditions and local port-specific processes such as vessel traffic, dredging, and local sediment resuspension. Therefore, the results should not be generalized too broadly. The main contribution of this study is the link between suspended-sediment variability and the practical screening of potentially challenging periods in port waters.

5.6 Limitations of the study

Several limitations should be considered when interpreting the results. First, the Seemannshöft analysis, including the temporal exceedance analysis, relied partly on estimated TSS values derived from the turbidity–TSS relationship. This approach extended the temporal analysis, but the regression had only moderate explanatory power. Therefore, the estimated TSS values should be treated as indicative values, not as exact replacements for direct TSS measurements.

The moderate R^2 value may partly reflect differences in temporal resolution and sampling between turbidity and TSS. Turbidity can vary over short timescales in an estuarine port, while TSS measurements are usually based on discrete water samples. By using daily averages, short-term peaks may have been smoothed, which could weaken the apparent turbidity–TSS relationship.

Therefore, the estimated TSS series should be interpreted as screening-level information. Future calibration should preferably be based on paired turbidity and TSS measurements from the same samples or from sampling times matched as closely as possible. Daily averaging may also have affected the identification of elevated estimated TSS event days, because short sub-daily peaks linked to tides, vessel manoeuvring, or local resuspension could have been smoothed below the 80 mg/L screening threshold.

A further limitation is that the turbidity–TSS regression was fitted with an intercept. A no-intercept model may be physically appealing, because zero turbidity would ideally correspond to zero suspended solids. However, the fitted-intercept model was retained as the empirical calibration based on the available paired observations. Future work could compare fitted-intercept and no-intercept calibrations as a sensitivity check. Seasonal regressions also indicated that the turbidity–TSS relationship differed between winter and summer. However, the annual regression was retained because it provided a consistent calibration for the full time series and because the seasonal subsets were relatively small.

The 80 mg/L threshold should not be interpreted as a ballast-water treatment limit. It was used only to flag clearly elevated estimated TSS conditions in the absence of a system-specific BWMS threshold. Therefore, exceedance days should be interpreted as screening-level indicators of potentially challenging water-quality conditions, not as confirmed operational exceedance events.

Because the maximum estimated TSS value was close to the 80 mg/L threshold, the exact number of exceedance days should be interpreted with caution and in relation to the threshold-sensitivity analysis. An exceedance of the 80 mg/L screening threshold should be interpreted as a signal of particle-rich conditions that may justify additional operational awareness or local checking, not as a direct indication of treatment failure.

A second limitation is the use of simple statistical relationships for the environmental drivers. Wind speed, air temperature, water level, and electrical conductivity were examined mainly through correlations and linear trends. This approach can show broad associations, but it cannot fully describe the interacting hydrodynamic, tidal, salinity-related, and sediment-transport processes in the lower Elbe.

Electrical conductivity was used as a salinity-related proxy because consistent direct salinity measurements were not available for the full study period. Conductivity can provide useful supporting information, but it is not the same as salinity. It was also available for fewer matched observations than the other environmental variables. Therefore, the conductivity results should be treated as supplementary evidence.

The satellite analysis was also limited by temporal data availability. The comparison between satellite-derived NDTI and in-situ observations depended on overlap between field measurements and cloud-free Sentinel-2 observations. As a result, the satellite–in-situ comparison had fewer matched observations than the turbidity-based estimated TSS analysis. The satellite results should therefore be interpreted as supportive, not as full validation of satellite-derived sediment estimates.

The spatial NDTI hotspot-frequency map also has limitations. The map was based on relative Sentinel-2-derived NDTI values and should not be interpreted as a direct TSS exceedance map. The hotspot-frequency values represent recurring elevated optical turbidity signals, not measured suspended-sediment concentrations. The results depend on the selected P95 threshold, mapped area, cloud filtering, water masking, valid-observation count threshold, and the 150 m smoothing step. Therefore, the map should be treated as a screening-level spatial product, not as a quantitative sediment concentration map or a direct BWMS risk map.

Although the temporal analysis covered 2018–2024, the study could not fully resolve long-term sediment dynamics or event-scale mechanisms.The data were useful for identifying multi-year patterns, seasonal tendencies, and episodic elevated estimated TSS conditions. However, they could not determine the exact physical causes of individual high-TSS events. Longer in-situ records, higher-frequency sediment measurements, and hydrodynamic or sediment-transport modelling would improve this.

Another limitation is that detailed hydrographic and channel-morphology data were not included as quantitative inputs. Such data are important in a port setting because water depth, channel geometry, navigation areas, and harbour infrastructure can influence local flow and sediment resuspension. HPA manages detailed hydrographic information for harbour management and navigation planning, but these datasets were outside the scope of the present analysis (Köster, 2017). Including them could improve the interpretation of local resuspension and spatial NDTI hotspot patterns.

Another limitation is that local port-operation drivers were not quantified. The goal document identified ship propeller-induced sediment resuspension in harbour basins as a possible local driver of elevated turbidity. In the present thesis, this process could only be addressed qualitatively. Quantitative assessment would require additional datasets such as AIS-based vessel traffic, vessel manoeuvring and berth-operation records, propeller and engine information, dredging activity logs, harbour-basin geometry, bed sediment characteristics, and high-frequency turbidity measurements close to ship-operation areas.

These data were not available within the scope of the thesis. As a result, the study cannot separate the effects of ship-induced resuspension from other local and estuarine processes such as tidal mixing, salinity-related flocculation, dredging disturbance, and upstream sediment supply.

The field visit provided only qualitative operational context. It helped explain why elevated TSS and particle-rich water may matter for ballast-water treatment operations, but it was not collected as a formal dataset and was not analysed quantitatively.

The log-transformed multiple regression and machine-learning analyses were exploratory and should not be interpreted as predictive models for operational use. The models were based on daily environmental variables and did not include higher-frequency tidal conditions, vessel traffic, dredging activity, particle-size information, or event-scale wastewater and stormwater inputs. The strong performance of lagged turbidity models mainly reflected temporal persistence in the turbidity record rather than a full explanation of the physical drivers.

The operational review was limited to regulatory context, industry-reported CWQ experience, and qualitative field-visit observations. Other local inputs, such as treated wastewater discharge, stormwater runoff, and combined sewer overflow, were not included because event-scale discharge and water-quality data were not available.

These limitations do not remove the value of the main findings, but they show where caution is needed. The study is strongest for identifying relative temporal patterns, seasonal tendencies, episodic elevated estimated TSS conditions, and supportive satellite-based spatial patterns. It is weaker for explaining the full physical mechanisms behind suspended-sediment dynamics or for building operational predictive models. Future work could use the station-based and satellite-based results to guide hydrodynamic, sediment-transport, or early-warning modelling by identifying relevant periods, locations, predictors, and data gaps.

In particular, the strong role of lagged turbidity suggests that future early-warning models should include recent local turbidity observations, while the limited explanatory power of the available environmental variables indicates that additional process-related data, such as tidal conditions, AIS-based vessel activity, dredging records, salinity, particle size, and high-frequency measurements, would be needed for more robust modelling.

5.7 Proposed Practical Framework for Assessing Challenging Water Quality

Based on the results of this thesis, a practical screening framework is proposed for assessing suspended-sediment-related challenging water quality conditions relevant to ballast water operations in the Port of Hamburg.

The framework is not intended to function as a regulatory decision tool or as a direct assessment of BWMS performance. Instead, it provides a structured way to combine local measurements, screening thresholds, environmental context, and satellite-derived spatial information.

From an operational perspective, the analysis is relevant because ballast-water uptake and treatment occur under local and time-varying port-water conditions. Elevated turbidity and TSS conditions may indicate particle-rich water, which can increase filtration demand, cleaning or backwashing needs, and general operational attention, depending on the BWMS design. Therefore, the temporal analysis of elevated TSS events and the spatial NDTI screening map can support operational awareness by indicating periods and areas where additional monitoring or caution may be useful. The results should not be interpreted as direct BWMS performance predictions or compliance assessments.

The framework follows five steps: local water-quality screening, threshold checking, environmental-context review, spatial screening, and operational caution. These steps are intended to support early screening and operational awareness, rather than automatic operational decisions.

The link between the environmental analysis and ballast water treatment is indirect but operationally relevant. The analyses identify suspended-sediment-related conditions that may require closer attention before or during ballast water uptake, especially for systems involving filtration and UV treatment. The framework therefore translates the thesis results into a screening logic for operational awareness, not into a prediction of treatment failure.

Table 5.2. *Practical screening framework for suspended-sediment-related challenging water quality.*

Step	Screening element	Indicator / data source	Interpretation	Practical implication
1	Local water-quality check	In-situ turbidity; measured or estimated TSS	Shows current local particle-rich conditions	Use local measurements as the primary screening basis
2	Threshold check	Measured or estimated TSS; 80 mg/L screening threshold or local percentile	Flags elevated suspended-sediment conditions	Treat exceedance as a warning signal, not a regulatory limit
3	Environmental context	Water level, discharge, conductivity, wind speed, air temperature	Provides supporting estuarine context	Use only as supporting context, not as a stand-alone predictor
4	Spatial screening	Sentinel-2-derived NDTI hotspot-frequency map	Identifies areas with recurring elevated optical turbidity signals	Prioritise areas for closer monitoring or awareness
5	Operational caution	Recent local measurements; BWMS-specific operating guidance	Links screening results to practical ballast-water operations	Consider increased caution, local checks, and uptake timing/location

In practical use, this framework would not automatically stop ballast water uptake or predict whether a ballast water management system will fail. Instead, an elevated screening signal would indicate that additional checks may be needed, such as reviewing recent local turbidity and TSS measurements, checking whether the uptake area overlaps with recurring high-NDTI zones, and considering relevant environmental context.

Local turbidity and TSS information form the primary basis for screening because they are directly linked to local water-quality conditions. Environmental variables and satellite-derived NDTI provide supporting context, but they should not be used alone to predict short-term turbidity or TSS peaks. The NDTI hotspot-frequency map should also be interpreted only as a relative optical screening layer, not as a direct TSS exceedance map or a BWMS risk map.

Operational decisions would still require recent local measurements, system-specific BWMS guidance, and port- or vessel-specific procedures. The main value of the framework is therefore not prediction of BWMS performance, but structured interpretation of available water-quality information before or during ballast-water-related operations.

Conclusions

This thesis assessed challenging water-quality conditions relevant to ballast-water operations in the Port of Hamburg, with a focus on suspended-sediment-related indicators at Seemannshöft during 2018–2024. The study used an observational, data-driven approach based on in-situ turbidity and TSS observations, environmental datasets, and Sentinel-2-derived NDTI. The aim was not to evaluate ballast water management system performance directly, but to identify water-quality conditions that may be relevant for ballast-water treatment, especially filtration and UV-based treatment.

A site-specific relationship between measured turbidity and measured TSS was developed using 118 matched observations. The relationship was positive but moderate, with $R^2 = 0.33$. This shows that turbidity can be used as a local indicator of TSS variability, but it does not fully explain measured TSS. For this reason, the estimated TSS values should be treated as indicative TSS-related values, not as exact replacements for direct TSS measurements.

The estimated TSS time series showed that suspended-sediment conditions at Seemannshöft were generally moderate, but interrupted by short elevated events. Monthly and seasonal analyses showed lower and more stable conditions during spring and summer, while autumn and winter had higher variability and more elevated values. This means that challenging conditions were expressed mainly through episodic peaks and seasonal variability, rather than through a smooth long-term trend.

Using 80 mg/L estimated TSS as a practical screening threshold, 16 exceedance days were identified out of 2244 daily values. This corresponds to 0.71% of the record. The maximum estimated TSS value was 88.37 mg/L and occurred on 13 January 2021. The 80 mg/L threshold was used only as a screening criterion and should not be interpreted as a regulatory limit, operational limit, or system-specific ballast-water treatment limit.

The analysis of environmental drivers showed that selected daily variables explained only part of the estimated TSS and turbidity variability. River discharge at Neu Darchau provided broader upstream hydrological context, but the comparison did not indicate a simple direct relationship with local estimated TSS at Seemannshöft. The log-transformed turbidity–TSS regression did not improve the calibration compared with the original linear model. Exploratory prediction analyses showed that recent turbidity observations were more informative for short-term turbidity prediction than individual daily environmental variables. Overall, these results suggest that suspended-sediment conditions were influenced by interacting estuarine, tidal, salinity-related, and local port-specific processes that could not be fully captured by the available daily variables.

Sentinel-2-derived NDTI provided useful supporting spatial information, but it could not replace in-situ measurements. NDTI showed weak positive relationships with measured turbidity and TSS/filter residue. The NDTI–turbidity comparison had more matched observations, while the NDTI–TSS comparison was limited to 15 exact-date matches. Therefore, the satellite analysis was interpreted as complementary spatial screening information, not as direct satellite-derived TSS.

The multi-year spatial NDTI hotspot-frequency analysis showed that recurring elevated optical turbidity signals were spatially heterogeneous across the port area. The P95 hotspot-frequency map provided screening-level information on areas where elevated NDTI conditions occurred more frequently during 2018–2024. However, these spatial hotspots should be interpreted as relative optical turbidity hotspots, not as direct TSS exceedance areas or direct measurements of suspended-sediment concentration.

A key outcome of the thesis is that environmental variables and satellite indicators can support screening, but they cannot replace direct local turbidity and TSS monitoring. The proposed framework should therefore be interpreted as a first screening step for identifying periods and areas where suspended-sediment conditions may become relevant to ballast-water operations. It is not a direct operational decision rule and does not assess system-specific treatment performance.

This study can be used as a first screening step within a broader monitoring–modelling framework. Historical NDTI hotspot-frequency maps could provide a spatial screening layer for identifying areas with recurring high or relatively low optical turbidity signals. Areas with consistently lower NDTI signals may indicate less turbid surface-water conditions, while areas with recurring high NDTI signals may require additional caution or in-situ verification before ballast-water uptake. However, NDTI alone cannot define ballast-water operation locations or treatment suitability.

Future work should combine satellite-based NDTI with fixed turbidity and TSS sensors, high-frequency in-situ measurements, particle-size information, AIS-based vessel activity, berth information, port-call records, Ballast Water Record Books, and detailed hydrographic and bathymetric data. This would allow satellite screening to be calibrated and validated locally and would provide a stronger basis for event-based screening, future modelling, and operational awareness.

The main relevance for ballast-water operations is that the thesis identifies particle-rich periods and areas where additional checks may be useful before ballast-water uptake. The study does not assess BWMS performance directly, but it provides an environmental screening basis that can support operational awareness and future decision-support tools.

References

International Maritime Organization (IMO). (2024). Resolution MEPC.387(81): Interim guidance on the application of the BWM Convention to ships operating in challenging water quality conditions. Adopted on 22 March 2024.

Bilotta, G. S., & Brazier, R. E. (2008). Understanding the influence of suspended solids on water quality and aquatic biota. Water Research, 42(12), 2849–2861. https://doi.org/10.1016/j.watres.2008.03.018

Copernicus Marine Service. (n.d.). Copernicus Marine Data Store. Retrieved April 29, 2026, from https://marine.copernicus.eu/

Casas-Monroy, O., Kydd, J., Rozon, R. M., & Bailey, S. A. (2022). Assessing the performance of four indicative analysis devices for ballast water compliance monitoring, considering organisms in the size range ≥10 to <50 µm. Journal of Environmental Management, 317, 115300. https://doi.org/10.1016/j.jenvman.2022.115300

Chen, W. B., Liu, W. C., & Hsu, M. H. (2015). Modeling investigation of suspended sediment transport in a tidal estuary using a three-dimensional model. Applied Mathematical Modelling, 39(9), 2570–2586. https://doi.org/10.1016/j.apm.2014.11.006

Chowdhury, M. M., et al. (2023). Monitoring turbidity in a highly variable estuary using Sentinel-2 for ecosystem management applications. Frontiers in Marine Science, 10, 1186441. https://doi.org/10.3389/fmars.2023.1186441

David, J., Gollasch, S., & David, M. (2026). International Maritime Organization, we may have a problem: Ballast water treatment triggers global concerns with antimicrobial resistant bacteria. Marine Pollution Bulletin, 226, 119277. https://doi.org/10.1016/j.marpolbul.2026.119277

Deutscher Wetterdienst. (n.d.). Climate Data Center. Retrieved April 29, 2026, from https://opendata.dwd.de/climate_environment/CDC/

Dong, K., Wu, W., Chen, J., Xiang, J., Jin, X., & Wu, H. (2023). A study on treatment efficacy of ballast water treatment system applying filtration plus membrane separation plus deoxygenation technology during shipboard testing. Marine Pollution Bulletin, 188, 114620. https://doi.org/10.1016/j.marpolbul.2023.114620

Duan, D., Xu, F., Wang, T., Guo, Y., & Fu, H. (2023). The effect of filtration and electrolysis on ballast water treatment. Ocean Engineering, 268, 113301. https://doi.org/10.1016/j.oceaneng.2022.113301

Dyer, K. R. (1997). Estuaries: A physical introduction (2nd ed.). John Wiley & Sons.

EMODnet. (n.d.). EMODnet Bathymetry. Retrieved April 29, 2026, from https://emodnet.ec.europa.eu/en/bathymetry

FGG Elbe. (n.d.). Fachinformationssystem der FGG Elbe. Retrieved April 29, 2026, from https://www.fgg-elbe.de/

Global Runoff Data Centre. (n.d.). River discharge data: Neu Darchau station. Federal Institute of Hydrology (BfG). Retrieved April 29, 2026, from https://www.bafg.de/GRDC/

Gorelick, N., Hancher, M., Dixon, M., Ilyushchenko, S., Thau, D., & Moore, R. (2017). Google Earth Engine: Planetary-scale geospatial analysis for everyone. Remote Sensing of Environment, 202, 18–27. https://doi.org/10.1016/j.rse.2017.06.031

Griffiths, W. H., & Walton, B. D. (1978). The effects of sedimentation on the aquatic biota. AOSERP Report 35. Alberta Oil Sands Environmental Research Program.

Grabemann, I., & Krause, G. (2001). On different time scales of suspended matter dynamics in the Weser Estuary. Estuaries, 24(5), 688–698. https://doi.org/10.2307/1352877

Hamburg Port Authority. (n.d.). Hamburg Port Authority. Retrieved April 29, 2026, from https://www.hamburg-port-authority.de/en/

Hamburg Port Authority. (2024). Wassertiefeninstandhaltung im Hamburger Hafen: Jahresbericht 2024. Tideelbe in Hamburg. Available at: https://www.tideelbe.info/fileadmin/user_upload/Downloads/Berichte/WTI-Jahresbericht_2024_fg.pdf

He, Z., Xue, M., Wang, Y., et al. (2026). Evaluation efficacy of filtration + UV-C radiation for ballast water treatment at different salinity. Journal of Environmental Management, 401, 128921. https://doi.org/10.1016/j.jenvman.2026.128921

Hesse, R. F., Zorndt, A., & Fröhle, P. (2019). Modelling dynamics of the estuarine turbidity maximum and local net deposition. Journal of Soils and Sediments, 19, 3780–3794. https://doi.org/10.1007/s11368-019-02393-1

INTERTANKO. (2026). Database on the experience of ships in ports with challenging water quality. MEPC 84/INF.32. Marine Environment Protection Committee, International Maritime Organization.

International Maritime Organization. (2018). Code for approval of ballast water management systems (BWMS Code) (Resolution MEPC.300(72)). International Maritime Organization.

International Commission for the Protection of the Elbe River (IKSE). (n.d.). The Elbe. Retrieved June 8, 2026, from https://www.ikse-mkol.org/en/themen/die-elbe

Köster, F. (2017). Centralised Data for Hamburg Port Authority: From Ping to Chart. Hydro International. Retrieved from https://www.hydro-international.com/case-study/centralised-data-for-hamburg-port-authority

Lee, M.-C., & Stenstrom, M. K. (2023). Water quality mitigation strategy analysis of the Salton Sea, California, using the Delft-3D modeling suite. Frontiers in Sustainable Resource Management, 2, 1178038. https://doi.org/10.3389/fsrma.2023.1178038

Lee, C. M., Hestir, E. L., Tufillaro, N. B., & Kuehl, J. J. (2021). Monitoring turbidity in San Francisco Estuary and Sacramento–San Joaquin Delta using satellite remote sensing. Journal of the American Water Resources Association, 57(5), 737–751. https://doi.org/10.1111/1752-1688.12917

Liu, J., Zhang, T., Wu, H., Li, L., Ren, J., & Qiu, C. (2023). Suspended sediment transport and turbidity maximum in a macro-tidal estuary with mountain streams: A case study of the Oujiang Estuary. Continental Shelf Research, 255, 104924. https://doi.org/10.1016/j.csr.2023.104924

Lloyd's Register. (2018). Ballast water management: Understanding your obligations. Lloyd's Register Group Limited.

Nangir, D., et al. (2025). Assessing the feasibility of satellite-based machine learning for turbidity estimation in the dynamic Mersey Estuary: Case study River Mersey, UK. Remote Sensing, 17(21), 3617. https://doi.org/10.3390/rs17213617

North, E. W., Chao, S. Y., Sanford, L. P., & Hood, R. R. (2004). The influence of wind and river pulses on an estuarine turbidity maximum: Numerical studies and field observations in Chesapeake Bay. Estuaries, 27, 132–146. https://doi.org/10.1007/BF02803567

Ohle, N., Shaikh, S., Thies, T., Strotmann, T., & Schmekel, U. (2023). Monitoring of suspended matter with H-ADCP devices and comparison with sedimentation rates and soil properties in the Köhlfleethafen harbour basin of the Hamburg port. EGU General Assembly 2023, Vienna, Austria, 24–28 April 2023, EGU23-14726. https://doi.org/10.5194/egusphere-egu23-14726

Outinen, O., Bailey, S. A., Casas-Monroy, O., Delacroix, S., Gorgula, S., Griniene, E., Kakkonen, J. E., & Srebaliene, G. (2024). Biological testing of ships' ballast water indicates challenges for the implementation of the Ballast Water Management Convention. Frontiers in Marine Science, 11, 1334286. https://doi.org/10.3389/fmars.2024.1334286

Port of Hamburg. (n.d.). Tides in the river Elbe. Retrieved June 8, 2026, from https://www.hafen-hamburg.de/en/portofhamburg/tide/

QGIS Development Team. (n.d.). QGIS Geographic Information System, version 3.40 Bratislava. Open Source Geospatial Foundation. https://qgis.org

Torres-Bejarano, F. M., Torregroza-Espinosa, A. C., et al. (2025). Modeling sediment transport and salt stratification in river estuaries: A case study of the Magdalena River, Colombia. Catena, 261, 109589. https://doi.org/10.1016/j.catena.2025.109589

Tideelbe. (n.d.). The Elbe: A river in the rhythm of the tides. Retrieved June 8, 2026, from https://www.tideelbe.info/en/under-water/the-elbe-a-river-in-the-rhythm-of-the-tides

U.S. Environmental Protection Agency. (2006). Developing water quality criteria for suspended and bedded sediments (SABS): Potential approaches. Office of Water.

Wan, Y., & Wang, L. (2018). Study on the seasonal estuarine turbidity maximum variations of the Yangtze Estuary, China. Journal of Waterway, Port, Coastal, and Ocean Engineering, 144(4), 05018002. https://doi.org/10.1061/(ASCE)WW.1943-5460.0000442

Wang, Q., Yu, X., Zhang, T., Du, J., & Wu, H. (2025). Towards more effective ship ballast water monitoring: Evaluating and improving compliance monitoring devices (CMDs). Water, 17(19), 2845. https://doi.org/10.3390/w17192845

Winterwerp, J. C., & van Kesteren, W. G. M. (2004). Introduction to the physics of cohesive sediment dynamics in the marine environment. Elsevier. https://doi.org/10.1016/S0070-4571(04)80004-9

Zhu, C., van Maren, D. S., Guo, L., Lin, J., He, Q., & Wang, Z. B. (2021). Effects of sediment-induced density gradients on the estuarine turbidity maximum in the Yangtze Estuary. Journal of Geophysical Research: Oceans, 126(5), e2020JC016927. https://doi.org/10.1029/2020JC016927

Appendix

Appendix A: Overview of datasets used in the thesis

Table A1. *Overview of the main datasets used for the observational assessment of challenging water quality conditions.*

Dataset	Source	Station / area	Period	Role in thesis
Turbidity	FGG Elbe	Seemannshöft	2018–2024	Main input for estimating TSS
TSS / filter residue	FGG Elbe	Seemannshöft	2018–2024	Calibration of turbidity–TSS regression
Electrical conductivity	FGG Elbe	Seemannshöft	2018–2024	Salinity-related proxy
Water level	HPA HydroOnline	Seemannshöft	2018–2024	Local tidal / hydrological context
River discharge	GRDC	Neu Darchau	2018–2024	Upstream hydrological context
Air temperature	DWD	Hamburg-Fuhlsbüttel	2018–2024	Meteorological / seasonal context
Wind speed	DWD	Hamburg-Fuhlsbüttel	2018–2024	Meteorological context
Sentinel-2 NDTI	Google Earth Engine / Sentinel-2	Port of Hamburg / Seemannshöft polygon	2018–2024	Relative optical and spatial screening
Spatial mapping	QGIS	Port of Hamburg	2018–2024	Map production and spatial outputs
Bathymetry / background data	EMODnet / background sources	Lower Elbe/Hamburg port	Reviewed	Background context only

Appendix B: Supplementary diagnostics for the log-transformed turbidity and prediction analyses

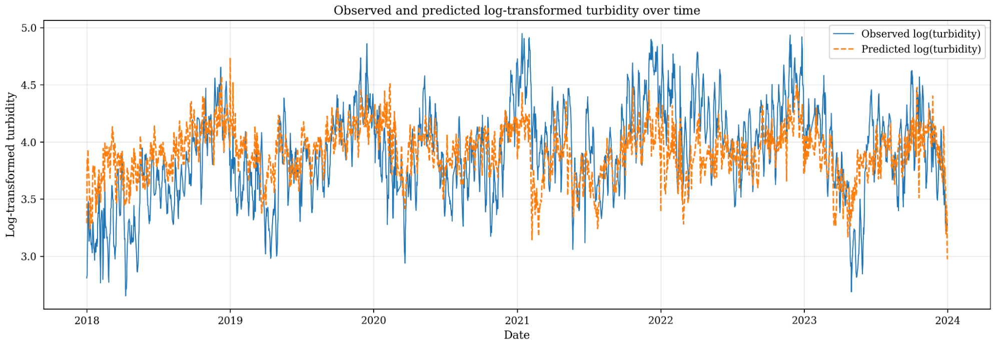

Figure B1. *Observed and predicted log-transformed turbidity over time from the multiple regression model using daily mean air temperature, wind speed, water level, and Neu Darchau discharge as predictors. The predicted series follows some broad temporal variability but does not consistently capture short-lived peaks and rapid changes, indicating limited predictive skill for event-scale turbidity variability.*

Table B1. *Summary of the matched dataset used for the log-transformed turbidity analysis. The dataset includes only dates with available turbidity, air temperature, wind speed, water level, and Neu Darchau discharge observations. Missing values refer to the final matched dataset after filtering.*

Item	Value
Matched observations	2113
Period	2018-01-01 to 2023-12-31
Missing values after matching	0
Missing dates in period	78
Response variable	log-transformed turbidity
Predictors	air temperature, wind speed, water level, discharge

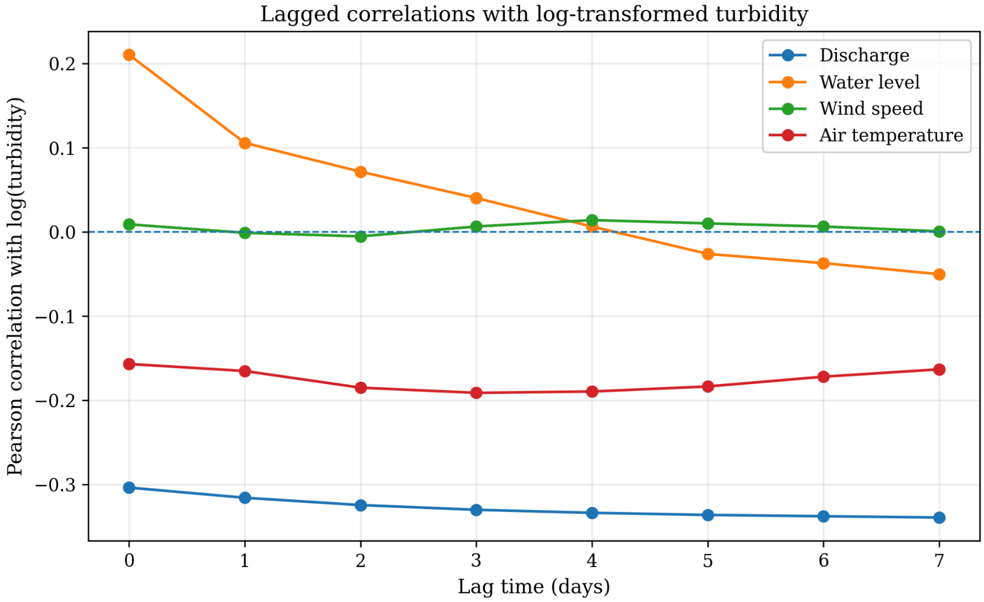

Figure B2. *Lagged Pearson correlations between log-transformed turbidity and selected environmental variables for lag times from 0 to 7 days. Discharge showed the strongest lagged association, with the highest absolute correlation at a 7-day lag, while water level was most strongly associated with same-day turbidity. Wind speed showed almost no lagged relationship.*

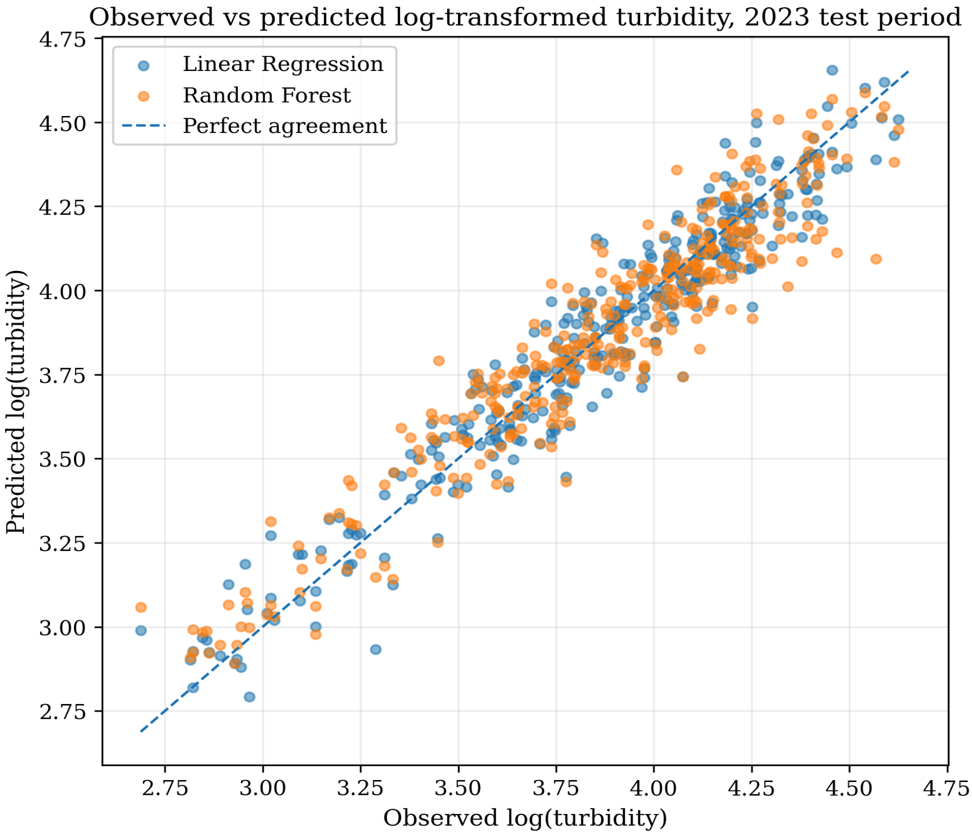

Figure B3. *Observed versus predicted log-transformed turbidity for the 2023 test period using Linear Regression and Random Forest models with lagged variables. The close agreement with the 1:1 line indicates strong short-term predictability when previous turbidity observations are included.*

Table B2. *PCA explained variance for environmental variables*

Principal component	Explained variance (%)	Cumulative explained variance (%)
PC1	41.7	41.7
PC2	30.3	72.0
PC3	15.8	87.8
PC4	12.2	100.0

Table B3. PCA loadings for environmental variables

Variable	PC1	PC2	PC3	PC4
temp_mean_C	-0.540	0.480	-0.096	0.685
wind_mean_ms	0.482	0.476	0.721	0.148
water_level_mean_cm	0.356	0.653	-0.615	-0.263
discharge_m3s	0.592	-0.343	-0.305	0.663

Table B4. *Random Forest forecast-window comparison using past 7-, 14-, and 21-day input windows to predict log-transformed turbidity 1, 2, and 3 days ahead. The model inputs were lagged log-transformed turbidity, air temperature, wind speed, water level, discharge, and rainfall. Training data covered 2018–2021, validation data covered 2022, and the independent test period was 2023.*

Input window	Horizon	Features	Val. R^2	Val. RMSE	Val. MAE	Test R^2	Test RMSE	Test MAE
7	1	42	0.637	0.187	0.147	0.784	0.184	0.146
7	2	42	0.396	0.241	0.195	0.715	0.211	0.175
7	3	42	0.236	0.271	0.221	0.618	0.245	0.201
14	1	84	0.692	0.172	0.134	0.791	0.180	0.142
14	2	84	0.550	0.208	0.166	0.728	0.206	0.168
14	3	84	0.464	0.227	0.179	0.666	0.229	0.189
21	1	126	0.708	0.168	0.131	0.779	0.186	0.147
21	2	126	0.566	0.204	0.163	0.707	0.214	0.174
21	3	126	0.491	0.221	0.174	0.658	0.231	0.188